IEEE Access
Multidisciplinary | Rapid Review | Open Access Journal

Received 16 May 2023, accepted 29 May 2023, date of publication 7 June 2023, date of current version 14 June 2023.

Digital Object Identifier 10.1109/ACCESS.2023.3283575

RESEARCH ARTICLE

Protection of the Future Harbor Area AC Microgrids Containing Renewable Energy Sources and Batteries

AUSHIQ ALI MEMON, (Member, IEEE), AND KIMMO KAUHANIEMI, (Member, IEEE)
School of Technology and Innovations, University of Vaasa, 65200 Vaasa, Finland

Corresponding author: Aushiq Ali Memon (amemon@uwasa.fi)

This work was supported by the Future Energy Storage Solutions in Marine Installations (FESSMI) Research Project funded by the European Regional Development Fund (ERDF) through the Finnish Funding Agency for Technology and Innovation (Tekes) under Grant 3345/31/2015.

ABSTRACT A significant share of global carbon emissions is related to marine vessels running solely on fossil fuels. The hybrid or fully electrified marine vessels using battery energy storage systems (BESS) both for onboard propulsion system and for cold-ironing during docking at harbor areas will significantly reduce marine related carbon emissions. However, the transformation of marine vessels' operations from diesel engines to BESS will necessarily require charging stations and other electric power infrastructure at harbor areas. The sustainable and cheap energy of renewable energy sources like wind turbine generators (WTGs), photovoltaic (PV) systems and related BESS could be used at harbor areas for charging depleted vessel-BESS and supplying power to cold-ironing loads. For this purpose, two new harbor area smart grid or AC microgrid models have been developed by our research group. This paper presents a comprehensive analysis of three-phase short-circuit faults for one of the proposed AC microgrid models using PSCAD/EMTDC simulations. The fault study of harbor area AC microgrid-1 is done for both grid-connected and islanded modes. The main purpose of the fault study is to check if grid-connected mode overcurrent settings of intelligent electronic devices (IEDs) will also be valid for different islanded mode fault cases with different fault current contributions from converter-based distributed energy resources (DERs) including WTG, PV and BESS. The extent of fault current contribution from DERs and BESS to avoid adaptive protection settings and to ensure definite-time protection coordination and fast fuse operations during different islanded modes is investigated.

INDEX TERMS Adaptive overcurrent protection, batteries, converter-based DERs, fuse, harbor area ac microgrids, islanded mode, renewable energy sources, short-circuit faults.

I. INTRODUCTION

The battery energy storage systems (BESS) both installed onboard the vessel and offboard at harbor area provide a great opportunity for reduction of fossil fuel consumption, carbon emissions and marine pollution. The BESS installations near harbor areas will help utilize the renewable energy sources (RES) including wind turbine generators (WTGs) and photovoltaic (PV) systems up to their maximum available potential. The correctly dimensioned BESS can easily replace some or all of the diesel engines used to propel a particular type of the vessel. This will not only help improve the dynamic response of the vessel propulsion system but also increase the energy efficiency of the system. In order to achieve these goals, the required supporting infrastructure should be installed not only onboard the vessel but also in the harbor area reaching the quay. This supporting infrastructure include all necessary electrical installations supplying power to electrical propulsion systems onboard the vessel and the harbor area power supply system enabling the "shore-to-ship connection" [1] for providing power to vessel load during cold-ironing and in the future also supply power for charging the depleted vessel batteries. Furthermore, the harbor area grid can include RES and BESS, in that case we can call the system as *harbor area smart grid* (HASG) [2].

In this regard, two alternative HASG models have been developed by our research group incorporating the technical suggestions provided by all the FESSMI project

The associate editor coordinating the review of this manuscript and approving it for publication was Giambattista Gruosso.

partners: One alternative for overnight offboard slow charging of vessel-BESS and the other for onboard fast charging of vessel-BESS during cold-ironing [3]. Both solutions consider providing power to onboard ship load from the RES installed at the harbor area during the docking period. This paper is limited to the first alternative HASG-1 (Fig. 1) that is a seven-bus supply system consisting of two main-grid buses (110 kV and 20 kV), two harbor area buses (20 kV and 0.69 kV), one charger bus (0.69 kV), one port bus (0.69 kV) and one ship bus (6.6 kV). The 20 kV harbor bus is located at a distance of 5 km from the transformer-T1 substation (110 kV/20 kV) connecting the main grid with HASG-1 through a 5 km long cable. The three units of container-based vessel-BESS each of 2 MW rating are connected with the 0.69 kV charger bus. These container-based vessel-batteries are charged overnight with 0.1C slow charging rate (10 hours for full charge). The 0.69 kV charger bus is connected to the upstream 20 kV harbor bus through a 2.5 km long cable and a 20 kV/0.69 kV, 3 MVA step down transformer-T4. The PV generator of 1 MVA and a wind turbine generator (WTG) of 3 MVA are connected at the 20 kV harbor bus via 5 km and 10 km long cables, respectively. Each of the PV and WTG has its local BESS to balance the normal weather-related power fluctuations and each one of them has its own 0.69 kV/20 kV step up transformer for connection to 20 kV harbor bus. A local harbor area load of 1.5 MVA is also connected to the 20 kV harbor bus.

The main grid connection to the cold-ironing load of 2 MW, 6.6 kV with two different frequencies of 50Hz and 60 Hz is also provided via the 20 kV harbor bus. The main grid connection to cold-ironing load is provided in two voltage-conversion stages: 20/0.69 kV and 0.69/6.6 kV. A 5 MVA, 50 Hz transformer-T2 at the 20 kV harbor bus steps down the voltage to 0.69 kV for providing LV connection to a 2 MW, 50/60 Hz frequency converter at the 0.69 kV harbor bus. The LV frequency converter converts the supply frequency from 50 Hz to 60 Hz at the 0.69 kV port bus. A 3 MVA 50/60 Hz transformer-T3 at the 0.69 kV port bus steps up the voltage from 0.69 kV to 6.6 kV to match the voltage level of the cold-ironing load. The star-point of shore-side transformer-T3 is earthed via a 200 Ohm continuous rated neutral earthing resistor as per recommendations in [4] for a nominal voltage of 6.6 kV. The frequency of cold-ironing load depends on the type of the vessel, if it is a 50 Hz vessel then direct connection from 0.69 kV harbor bus to 0.69 kV port bus is provided without the need of a frequency converter in between these two buses.

A 2.5 km long cable at the secondary of 0.69/6.6 kV transformer-T3 is connected to the 6.6 kV ship bus. At 6.6 kV ship bus the 2 MW loads of 50 Hz and 60 Hz vessels are connected via a 0.2 km flexible-cable. A single 3 MVA transformer-T3 connection at 0.69/6.6 kV conversion stage dictates that only one type of vessel load either 50 Hz or 60 Hz can be supplied at a time. An additional 2 MVA BESS is also connected at 0.69 kV harbor bus, which can be used to supply cold-ironing load if connection to the main-grid and

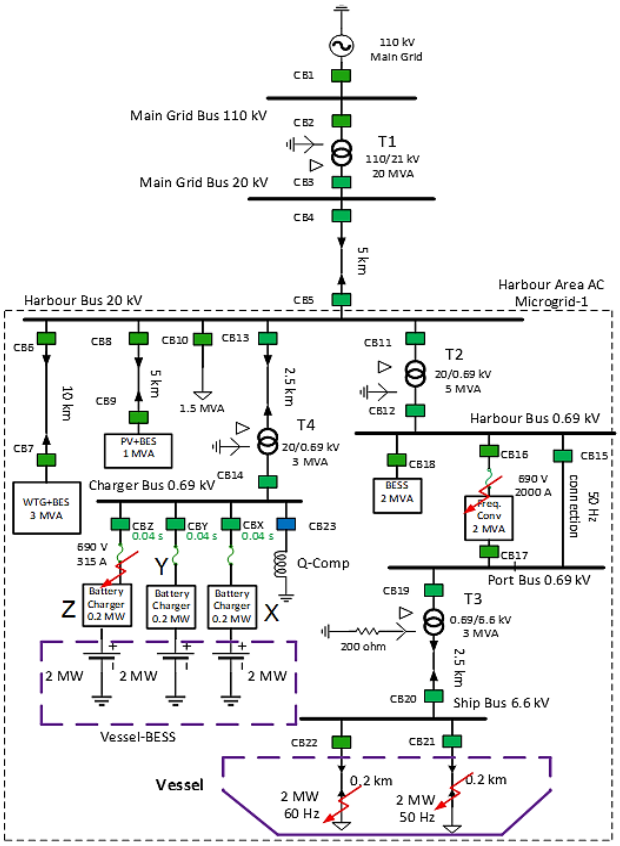

FIGURE 1. The first alternative HASG-1 model with renewable DERs and BESS (For 10 hour overnight slow charging of vessel-BESS).

distributed energy resources (DERs) is lost in case of fault at 20/0.69 kV transformer-T2. The main purpose of the DERs connected at the 20 kV harbor bus of HASG-1 is to supply charging power to container-based vessel-BESS at harbor area during night and supply power to cold-ironing load when empty container-based vessel-BESS are being replaced by charged batteries. Also, the harbor area load of 1.5 MVA connected at the 20 kV harbor bus has to be supplied by DERs depending on the available capacity. The main idea behind the HASG-1 is to use clean renewable energy available at harbor area up to its maximum available potential and reduce emissions by avoiding diesel generator operations during cold-ironing and use overnight charged batteries for hybrid vessel drives/propulsion system during the journey.

The proposed harbor area smart grid also considers importing the deficit power from the main grid if local DERs are not able to provide an adequate amount of power to cold-ironing load or vessel-BESS being charged plus local harbor area load and system losses. Normally, harbor area smart grid will be operated in grid-connected mode for a stable operation. However, during faults on the main grid, only DERs and BESS inside the harbor area smart grid will be available to supply power. In this situation, HASG-1 is said to be operating in the islanded mode. The overall structure of HASG-1 is like an AC microgrid with DERs, BESS and loads, that

can be operated in grid-connected or islanded mode. Therefore, the standards [5], [6], [7], and [8] for DERs and the standards [9] and [10] for AC microgrids are very much relevant to the proposed HASG-1 model in addition to the standards [4], [11], and [12] for ''shore-to-ship connection'' of marine installations. The main objective of this paper is to analyze remote three-phase short-circuit (SC) faults and investigate the operational suitability of traditional overcurrent (OC) protection schemes and fuses in the islanded mode of the proposed HASG-1 to be called from here onwards as *harbor area AC Microgrid-1* using PSCAD simulations.

The traditional protection schemes using single-setting definite-time and inverse-time OC relays, and fuses usually work quite well during the grid-connected mode of AC microgrid due to sufficient short-circuit current from the main grid. However, during the islanded mode more sensitive OC protection schemes are essentially required due to the limited available short-circuit current from DERs. It means adaptive OC settings are generally required for detection and isolation of faults in both grid-connected and islanded modes of AC microgrids with converter-based DERs [13], [14], [15], [16].

Due to the reduced/limited fault current contributions of DERs in the islanded mode, either the operation of fuse becomes very slow, or the failure of fuse operation happens. Previously in [17], the operation of fuse was practically observed within an islanded microgrid in central Finland that was fed by 120 kVA back-to-back converter. The 32 A gG type of fuse cleared different types of faults within 300-500 ms with a fault current contribution of the converter equal to its rated current. However, the results presented did not mention the size of the load being protected by the fuse. Nevertheless, the operation of fuse was quite slow therefore unsuitable for the fast fault clearance and proper maintenance of protection coordination with other backup overcurrent protection relays. Recently, a modified overrated energy storage inverter design has been proposed in [18] that provides three times the rated full load current during three-phase short-circuit fault in the islanded microgrid. The results show that the fuse (12.5 A) blows/operates within 500 ms of the three-phase fault. Although the fuse-relay and relay-relay coordination are maintained, the coordination time interval (CTI) between the fuse and backup overcurrent relay is three-times longer than the usual 200 ms. The CTI for the relay-relay coordination is even six times longer than 200 ms. The impact of energy storage devices on the control and protection system when used together with the RES generators was studied earlier in [19]. This paper diagnosed a considerable variation of fault current from the storage devices when suddenly switching from the generator mode to the load mode and vice versa. Therefore, adaptive protection scheme was suggested. Due to the lack of suitable simulation models of energy storage devices, the detailed protection coordination and fault dynamics were not analyzed.

Majority of the previous papers have only focused on the detection of short-circuit fault current and then limiting the output current of converter-based DERs to the rated current or below it either using the fault current limiters (FCL) or by adjusting the control of converters. In [20], the output current of the converter in a low voltage DC distribution network during the fault is limited by the control and then tripping is carried out within 50 ms using a non-standard controlled circuit breaker. A similar method is presented in [21] that utilizes current limiting control before isolation of different faults in an isolated AC microgrid with single DER unit. Fault detection and isolation are done using voltage and current thresholds followed by circuit breaker tripping. An output power and current limiting controls have been proposed in [22] for providing overload and overcurrent protection of directly voltage controlled DERs in an AC microgrid.

In [23], the protection of a looped AC microgrid is proposed using simple inverse-time OC devices with the same settings. The DERs close to the fault are controlled in a manner to inject relatively larger current than other DERs proportional to the measured impedance of the microgrid. The detection of the fault is based on indirect measurement of microgrid impedance. The supercapacitors of reduced sizes are used at the DC links of DER inverters for the enhancement of the fault current. Although, the results show a proper coordination between two OC devices at both ends of the fault, the backup protection is provided with either too small or too large values of CTI. Consequently, the OC devices other than the required are tripped without isolating the fault when primary OC devices fail to operate. General factors and requirements affecting the fault interruption and protection coordination for AC, DC and hybrid microgrids in distribution systems with converter-based DERs are discussed in [24]. The protection scheme for hybrid low voltage AC/DC distribution system is proposed in [25]. The proposed scheme uses high-speed DC circuit breaker for faults in remote DC section and recloser scheme using AC circuit breakers for faults in AC section near utility transformer. This way protection coordination is established between the protection devices. In our previous work [14], it was found that definite-time OC relays perform better than inverse-time OC relays for the remote faults in the grid-connected mode of AC microgrid. The performance of definite-time OC relays in terms of operating time and CTI between relays was even better during faults in the islanded mode with grid-forming BESS and grid-following DERs. However, the operation of fuse was not considered in that study.

The literature review indicates that there is still a research gap for the global protection coordination study in the islanded mode of AC microgrid. Particularly, due to the increasing applications of BESS along with the RES for an operational flexibility. This new phenomenon can enhance fault levels in distribution networks and microgrids. Additionally, with ever-increasing penetration levels of DERs the future grid codes are expected to demand large converter sizes or extra fault current sources for providing more than the

rated current during faults, particularly in the islanded mode of operation.

The evaluation of adaptive protection of AC microgrid using the current-limiting grid-following and grid-forming controls of converter-based DERs during the grid-connected and islanded modes was done in our previous paper [15] with 1.2 p.u. fixed fault current contribution. In this paper, the increased fault current contributions of converter-based DERs (1.2 p.u. and greater) are evaluated to check whether adaptive protection can be avoided in the islanded modes of AC microgrid. The details about various types of grid-forming controls of converter-based DERs can be found in [26] and [27]. In this paper, generic PSCAD-based models of grid-forming and grid-following converter-based DERs have been used. The converter-based DER models employ dq-control with inner current loop and outer power loop. The grid-forming control is implemented using voltage-controlled oscillator (VCO) in the islanded mode. The load and generation are closely balanced during islanded modes for voltage and frequency regulation. The maximum overcurrent during faults is limited by using a saturator block. The used grid-forming control is simplified version of the control presented in [28].

Considering the above factors, the focus of this paper is on the islanded-mode fault cases with different fault current limiting scenarios of DERs and BESS. Nevertheless, selected fault cases for the grid-connected mode are also presented for comparisons. In this regard, maximum load current at each OC relay has been found in different grid-connected and islanded modes of the considered harbor area AC microgrid-1. Then following questions have been addressed:

- What will be the magnitude of fault current at each OC relay during the remote three-phase SC faults in different grid-connected and islanded modes of the considered AC microgrid-1?
- In which fault cases of islanded mode operation and at what fault current levels of converter-based DERs and BESS the protection coordination and fuse operation will be ensured, and adaptive OC protection be avoided by using the same grid-connected mode definite-time OC settings of relays?

The rest of the paper is organized in a way that Section II presents the detailed fault study and evaluation of OC protection of the proposed harbor area AC microgrid-1 during both grid-connected and islanded modes with different scenarios of fault current contributions of DERs and BESS. Section III includes discussion and summary of results and Section IV concludes the paper.

II. FAULT STUDY AND EVALUATION OF PROTECTION OF THE HARBOR AREA AC MICROGRID-1

The operational modes of the proposed harbor area AC microgrid-1 (Fig. 1) can be broadly divided into two categories: (1) Grid-connected mode (2) Islanded mode. Each of the two mentioned operational modes can be subdivided into two further modes: (a) Slow-charging of container-based vessel-BESS during night with no cold-ironing load; (b) Power supply to cold-ironing load with no slow-charging of the container-based vessel-BESS. Again, during the power supply to cold-ironing load, it should be considered if the vessel type/load type is 50 Hz or 60 Hz.

If vessel type/load type is 60 Hz, then it has to be supplied through the frequency converter that can only provide fault current up to twice the magnitude of the nominal current for a duration of *two* seconds [29] or less for faults at and downstream of 0.69 kV port bus in both grid-connected and islanded modes of operation. Therefore, irrespective of grid-connected or islanded mode of operation, all OC protection relays or IEDs (intelligent electronic devices) downstream of the frequency converter need to be more sensitive for 60 Hz cold-ironing load/vessel type.

On the other hand, for the 50 Hz cold-ironing load the OC protection IEDs will need different settings for grid-connected and islanded modes. The islanded-mode settings will greatly depend upon the short-circuit current from DERs and BESS. The number of OC protection IEDs is equal to number of circuit breakers (CBs) at various locations in Fig. 1 and each CBxx is operated by the related IED referred later in this paper as IEDxx. The frequency converter and battery chargers are primarily protected with fast acting fuses and local OC protection IEDs act as backup for fuses. In this paper, only the OC function has been considered for the proposed AC microgrid-1 (Fig. 1), therefore all IEDs referred to in the following subsections are OC protection IEDs with definite-time coordination. The fault analysis and tripping response of OC devices for different operational modes are given in the following subsections.

A. FAULTS DURING GRID-CONNECTED MODE

When the proposed harbor area AC microgrid-1 is operated in the grid-connected mode, the maximum fault current contribution has to come naturally from the main grid. The fault current contributions from DERs have to be minimum in the grid-connected mode for any downstream fault within AC microgrid or any upstream fault on the main grid. In order to find the maximum possible load current at each IED, all DERs including the 2 MVA BESS at 0.69 kV harbor bus are disconnected in the first step and the load currents at all IEDs are obtained with only the main-grid connected.

Table 1 shows magnitudes of load currents, I (A) and voltages, V_{ph-ph} (kV) at all IEDs except IEDs 6-10,13-14, 16-18 and 23 when all power is supplied from the main grid and only 50 Hz cold-ironing load and harbor bus load are connected. With the final voltage level of 0.96 p.u. at 2 MW, 50 Hz ship load terminal a peak load demand of 92.5% is met with these voltage settings due to an impedance-based voltage-dependent load.

Table 2 shows magnitudes of load currents and voltages at all IEDs except IEDs 6-10, 13-15, 18 and 23 when all power is supplied from the main grid and only 60 Hz cold-ironing

TABLE 1. Currents & voltages at IEDs when only the main grid supplies power to 50 Hz cold-ironing & harbor load (no DER mode).

IED#	I (A)	V_{ph-ph} (kV)	IED#	I (A)	V_{ph-ph} (kV)
IED1	18.96	110	IED12	1647.5	0.682
IED2	18.96	110	IED15	1644	0.682
IED3	100.4	20.33	IED19	1644	0.682
IED4	100.4	20.31	IED20	171.5	6.33
IED5	101.34	20.03	IED21	171.5	6.33
IED11	57.29	20.03			

TABLE 2. Currents & voltages at IEDs when only the main grid supplies power to 60 Hz cold-ironing & harbor load (no DER mode).

IED#	I (A)	V_{ph-ph} (kV)	IED#	I (A)	V_{ph-ph} (kV)
IED1	20.1	110	IED12	1825	0.687
IED2	20.1	110	IED16	1825	0.683
IED3	106.8	20.3	IED17	1748	0.725
IED4	106.8	20.3	IED19	1748	0.725
IED5	107.5	20.02	IED20	182.6	6.72
IED11	63.25	20.02	IED22	182.6	6.72

TABLE 3. Currents & voltages at IEDs when only the main grid supplies power to depleted vessel-BESS & harbor load (no DER mode).

IED#	I (A)	V_{ph-ph} (kV)	IED#	I (A)	V_{ph-ph} (kV)
IED1	11.84	110	IED13	18.63	20.2
IED2	11.84	110	IED14	540	0.694
IED3	62.67	20.4	IEDX	299	0.695
IED4	62.67	20.38	IEDY	299	0.695
IED5	63.16	20.2	IEDZ	299	0.695

load and harbor bus load are connected. With the final voltage level of 1.02 p.u. at the 2 MW 60 Hz ship load terminal a peak load demand of 100% is met with these voltage settings. This is possible due to increased voltage of 1.05 p.u. (0.725 kV/0.69 kV) at the output of frequency converter. Table 3 gives magnitudes of load currents and voltages at all IEDs except IEDs 6-12 and 15-23 when all power is supplied from the main grid and only container-based vessel-BESS and the harbor bus load are connected.

Table 4 and Table 5 show load currents and voltages at the active IEDs in case of power supply to 50 Hz and 60 Hz cold-ironing loads, respectively when both WTG and PV system are also operating in parallel to the main grid. Table 6 shows load currents and voltages in case of power supply to depleted vessel-BESS for slow charging during the night when only the WTG is operating in parallel to the main grid. In this case it is assumed that the PV system will be naturally out of service during the night and BES (battery energy storage) at PV system may not be available. Moreover, slow charging of the depleted vessel-BESS requires less power (0.6-0.75 MW) as compared to 2 MW for cold-ironing load. Therefore, it is not feasible to charge depleted vessel-BESS by BES at PV location even if sufficient storage is available until and unless the WTG is also out of service.

First, magnitudes of load currents during different operational modes are obtained by simulations as presented in Table 1-6. Then the maximum magnitude of load current ($I_{max-load}$) at each IED (green highlight) is selected from these calculations as the basis for OC settings. Pickup

TABLE 4. Currents & voltages at IEDs when the main grid, WTG and PV supply power to 50 Hz cold-ironing and harbor load.

IED#	I (A)	V_{ph-ph} (kV)	IED#	I (A)	V_{ph-ph} (kV)
IED1	2.12	110	IED9	27.44	20.59
IED2	2.12	110	IED11	58.7	20.5
IED3	16.7	20.48	IED12	1687.8	0.701
IED4	16.7	20.48	IED15	1682.9	0.701
IED5	12.93	20.5	IED19	1682.9	0.701
IED6	82.06	20.5	IED20	176.14	6.49
IED7	79.68	20.98	IED21	176.14	6.49
IED8	28.73	20.5			

TABLE 5. Currents & voltages at IEDs when the main grid, WTG and PV supply power to 60 Hz cold-ironing and harbor load.

IED#	I (A)	V_{ph-ph} (kV)	IED#	I (A)	V_{ph-ph} (kV)
IED1	3.51	110	IED9	27.43	20.6
IED2	3.51	110	IED11	64.8	20.5
IED3	24	20.5	IED12	1870	0.703
IED4	24	20.5	IED16	1870	0.699
IED5	20.2	20.517	IED17	1790	0.746
IED6	82.03	20.518	IED19	1790	0.746
IED7	79.65	21	IED20	187	6.9
IED8	28.72	20.518	IED22	187	6.9

TABLE 6. Currents & voltages at IEDs when the main grid and WTG supply power to depleted vessel-BESS and harbor load.

IED#	I (A)	V_{ph-ph} (kV)	IED#	I (A)	V_{ph-ph} (kV)
IED1	4.1	110	IED7	79.46	21.05
IED2	4.1	110	IED13	18.25	20.56
IED3	26.65	20.5	IED14	528.5	0.709
IED4	26.65	20.5	IEDX	303.75	0.708
IED5	23.42	20.56	IEDY	303.75	0.708
IED6	81.85	20.56	IEDZ	303.75	0.708

TABLE 7. Pickup current threshold settings of all considered IEDs.

IED#	I>>	I>	IED#	I>>	I>	IED#	I>>	I>
IED1	50.3	25.15	IED8	71.8	35.9	IED21	440.4	220.2
IED2	50.3	25.15	IED9	68.6	34.3	IED13	46.6	23.3
IED3	267	133.5	IED11	162	81	IED14	1350	675
IED4	267	133.5	IED12	4675	2338	IEDX	759.4	379.7
IED5	269	134.5	IED15	4207	2104	IEDY	759.4	379.7
IED6	205	102.5	IED19	4475	2238	IEDZ	759.4	379.7
IED7	199	99.6	IED20	467.5	234	-		

I>> Threshold of OC stage (A), I> Threshold of overload stage (A)

currents of all two-stage IEDs have been set at 2.5 times $I_{max-load}$ for OC stage (I≫) and 1.25 times $I_{max-load}$ for the overload stage (I>) as given in Table 7. The definite-time delay settings for all considered IEDs are given in Table 8. These delay settings of IEDs remain unchanged irrespective of the grid-connected or islanded mode. Relatively long time delays for IEDs related to DERs (Table 8 in red color) ensure required low voltage ride-through (LVRT) and remote backup protections for IEDs in the fault path. The DERs are set to provide fault currents up to 1.2 p.u. of base or rated current in the grid-connected mode.

1) THREE-PHASE FAULT AT 50 HZ COLD-IRONING LOAD WHEN SUPPLIED BY MAIN GRID, WTG AND PV

Protection settings of all active IEDs have been evaluated in this case during a 3-phase SC fault at 50 Hz cold-ironing

TABLE 8. Definite-time delay settings of all considered IEDs.

IED#	t_{op}	IED#	t_{op}	IED#	t_{op}
IED1	2.0	IED8	2.0	IED20	0.2
IED2	1.8	IED9	2.2	IED21	0.02
IED3	1.6	IED11	1.0	IED13	0.44
IED4	1.4	IED12	0.8	IED14	0.24
IED5	1.2	IED15	0.6	IEDX, Y, Z	0.04
IED6	2.0	IED18	2.0	FuseX, Y, Z	0.02
IED7	2.2	IED19	0.4	-	

t_{op} = Operating time (s)

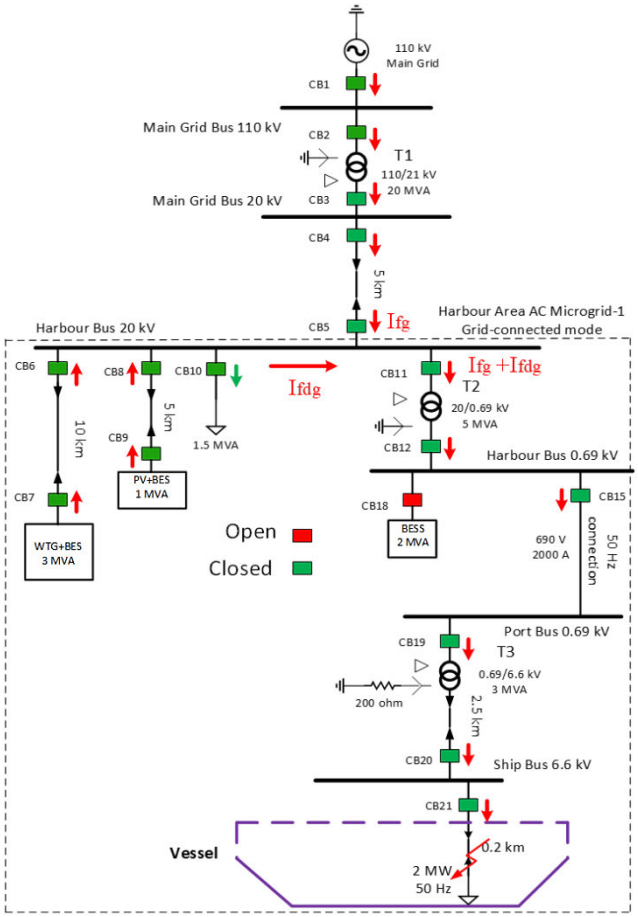

FIGURE 2. 3-phase short-circuit fault at 50 Hz cold-ironing load in grid-connected case-1.

load supplied by main grid, WTG and PV system (Fig. 2). A 3-phase SC fault is applied for a duration of 4 s, from the simulation time of 1.2 s to 5.2 s.

The rms magnitudes of fault currents at all active (green) IEDs for this case are given in Table 9. The fault current magnitudes at IEDs 1-5, 11-12, 15, 19-21 are well above the pickup settings of 2.5 x $I_{max-load}$ for OC stage of IEDs during the considered 3-phase fault. Therefore, not only the primary IED21 will pick up and trip but all upstream IEDs to IED21 will also pick up during 3-phase SC fault at 50 Hz cold-ironing load for providing backup protection in case of CB21 failure.

TABLE 9. Voltages and currents at active IEDs during 3-phase short-circuit fault at 50 Hz cold-ironing load in grid-connected case-1.

IED#	I (A)	V_{ph-ph} (kV)	IED#	I (A)	V_{ph-ph} (kV)
IED1	110.2	110	IED9	32.52	17.35
IED2	110.2	110	IED10	38.1	17.25
IED3	588	18.22	IED11	642	17.25
IED4	588	18.22	IED12	18580	0.413
IED5	591.5	17.25	IED15	18554	0.413
IED6	94.81	17.25	IED19	18561.5	0.413
IED7	92.95	17.8	IED20	1937.47	0.0975
IED8	33.55	17.25	IED21	1937.47	0.011

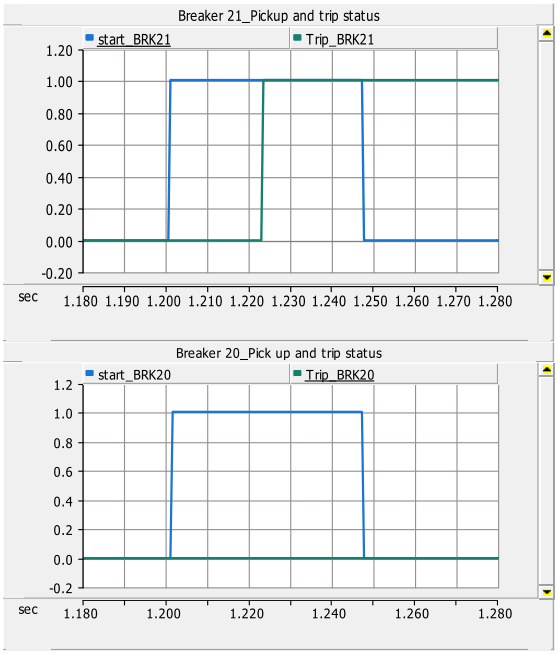

FIGURE 3. Pickup (start) and tripping status of primary IED21 & backup IED20 during 3-phase SC fault at 50 Hz cold-ironing load in grid-connected case-1 (start_BRK21 = pickup signal for IED21, trip_BRK21 = tripping status of IED21 with status 0 = closed and status 1 = open).

The pickup and tripping status signals of primary IED21 and the first backup IED20 are shown in Fig. 3. It can be observed from Fig. 3 that IED21 trips within the required 20 ms of 3-phase SC fault and backup IED20 also picks up.

The rms magnitude of fault current per phase at IED21 is shown in Fig. 4. The fault current contribution from DERs during 3-phase SC fault at 50 Hz cold-ironing load is lower than the current limiter setting (I-lim) of 1.2 p.u. of base current (Fig. 5) that is calculated at the rated voltage and rated power capacity of the DER. Therefore, IEDs 6-9 can only see the fault currents up to 1.15-1.18 times $I_{max-load}$ and these will neither pick up nor trip falsely for this fault case in grid-connected case-1.

2) THREE-PHASE FAULT AT CHARGER-Z TERMINAL WHEN SUPPLIED BY MAIN GRID AND WTG

The protection settings of all active IEDs have been evaluated in this case during a 3-phase SC fault at charger-Z terminal when supplied by main grid and WTG (Fig. 6). The rms

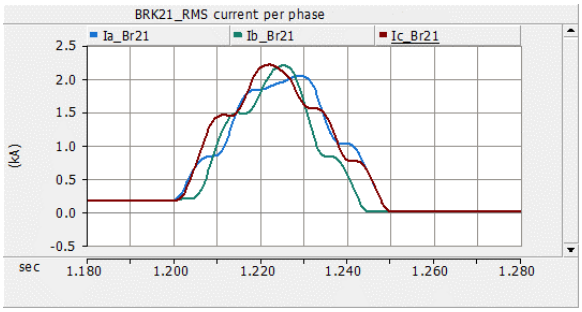

FIGURE 4. Magnitude of current per phase of primary IED21 during 3-phase SC fault at 50 Hz cold-ironing load in grid-connected case-1 (Ia_Br21, Ib_Br21, Ic_Br21 = line currents at IED21).

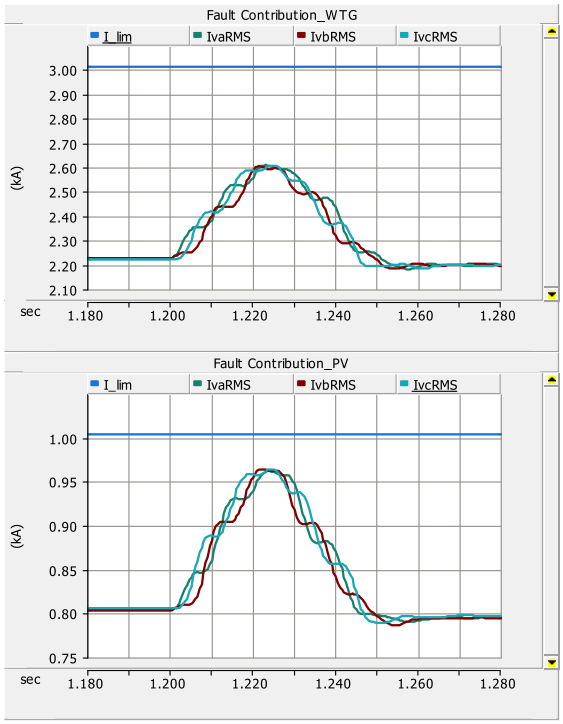

FIGURE 5. Magnitude of fault current contribution per phase by WTG and PV system during a 3-phase SC fault at 50 Hz cold-ironing load in grid-connected case-1 (I_lim = Current limiter setting of the DER, IvaRMS, IvbRMS, IvcRMS = Line currents at LV terminals of DERs).

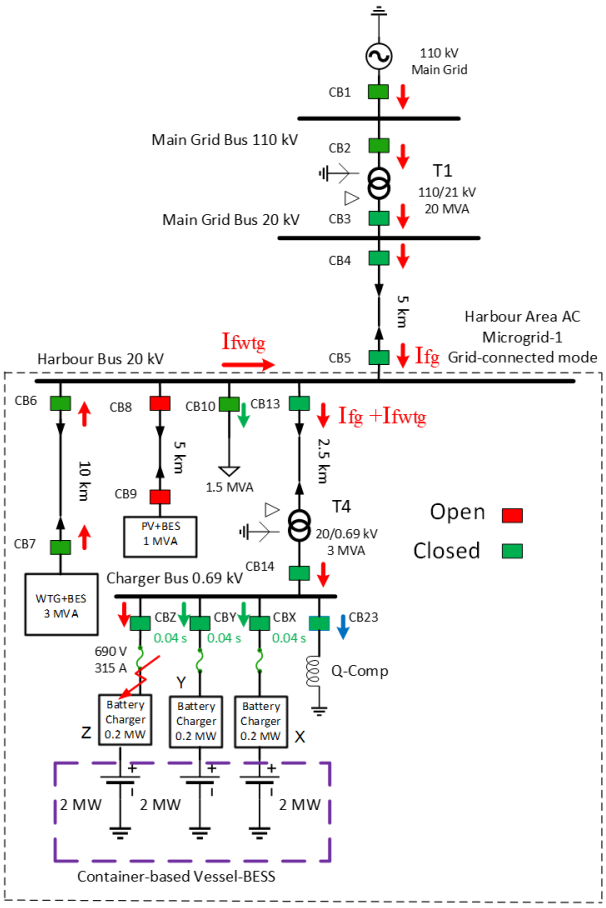

FIGURE 6. 3-phase short-circuit fault at charger-Z terminal in grid-connected case-2.

TABLE 10. Voltages and currents at active IEDs during 3-phase short-circuit fault at charger-Z terminal in grid-connected case-2.

IED#	I (A)	$V_{ph\text{-}ph}$ (kV)	IED#	I (A)	$V_{ph\text{-}ph}$ (kV)
IED1	213	110	IED10	30.7	14.3
IED2	213	110	IED13	1210	13.88
IED3	1144	16.95	IED14	35100	0.204
IED4	1144	16.95	IEDX	100	0.26
IED5	1145	14.3	IEDY	100	0.26
IED6	105	14.5	IEDZ	35000	decay to zero
IED7	103.5	13.9			

magnitudes of fault currents at all active IEDs are given in Table 10. The fault current magnitudes at IEDs 1-5, 13-14 and IEDZ are well above pickup settings of 2.5 x $I_{max-load}$ for OC stage of IEDs during the considered 3-phase SC fault. Therefore, not only the primary IEDZ will pick up and trip but all upstream IEDs to the IEDZ will also pick up during a 3-phase SC fault at charger-Z terminal and provide backup protection in case of CBZ failure.

The rms magnitude of fault current per phase at IEDZ during 3-phase SC fault at charger-Z terminal is shown in Fig. 7. The pickup and tripping status signals of primary IEDZ and the nearest/first remote backup of IEDZ, that is, IED14 are shown in Fig. 8. It can be seen from Fig. 8 that the IEDZ opens CBZ within the required delay of 40 ms after the fault. The pickup status of IED14 shows that it will act as a backup for IEDZ if CBZ fails to open. It should be noted that the IEDs X, Y, and Z act as backups for the fast acting fuses at these locations and these are coordinated with fuses with a coordination delay of 20 ms. The fast acting fuseZ blows within 20 ms of the 3-phase SC fault (Fig. 9).

The fault current contribution per phase from the WTG operating in parallel to the main grid during a 3-phase SC fault at charger-Z terminal is shown in Fig. 10. The WTG supplies the fault current contribution up to the current limiter setting (I-limit) of 1.2 p.u. of base current during this scenario. The IED6 and IED7 can sense the fault current magnitude of about 1.3 × $I_{max-load}$ (compared with Table 6 values) that is less

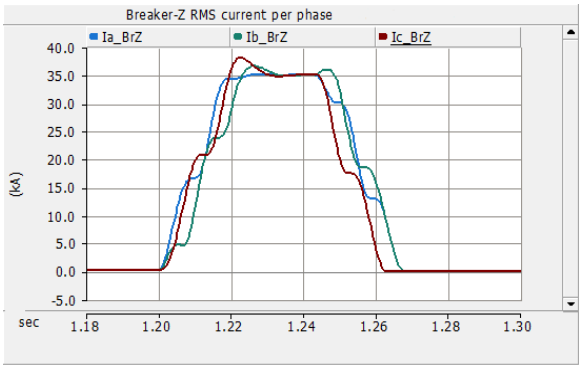

FIGURE 7. Magnitude of current per phase of IEDZ during 3-phase SC fault at charger-Z terminal in grid-connected case-2 (Ia_BrZ, Ib_BrZ, Ic_BrZ = line currents at IEDZ, Br = BRK = breaker).

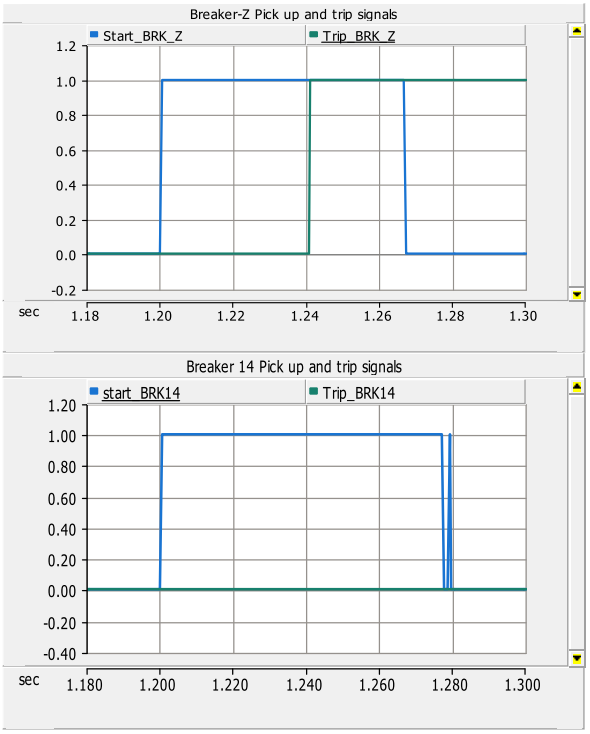

FIGURE 8. Pickup and tripping status of primary IEDZ and backup IED14 during 3-phase SC fault at charger-Z terminal in grid-connected case-2.

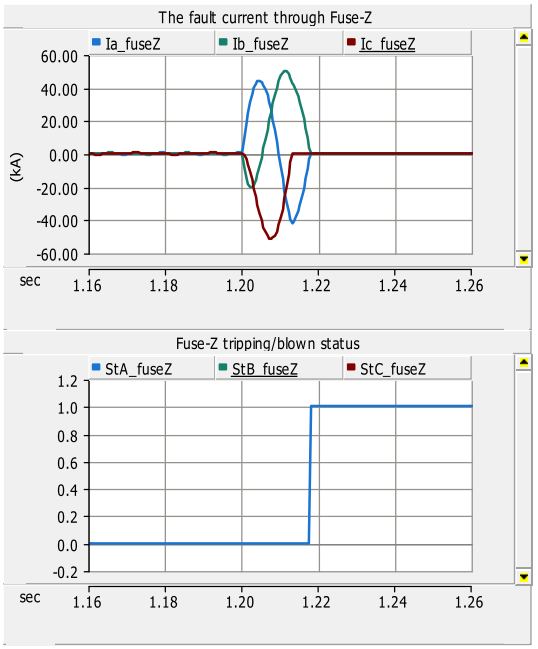

FIGURE 9. Magnitude of current per phase through fuseZ and its tripping/blown status during 3-phase SC fault at charger-Z terminal in grid-connected case-2 (StA_fuseZ = status of fuse, 1 = open, 0= closed).

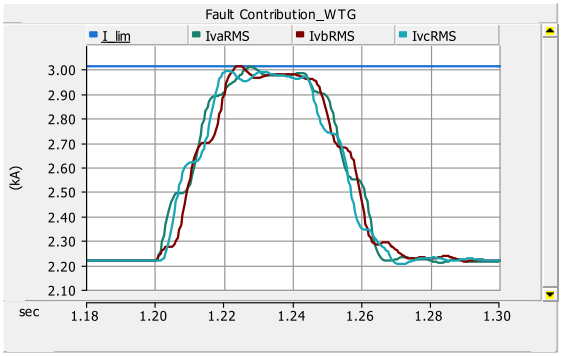

FIGURE 10. Magnitude of fault current contribution per phase by WTG during 3-phase SC fault at charger-Z terminal in grid-connected case-2.

than the set OC stage limit of 2.5 $\times$ $I_{max-load}$. Hence no OC pickup and nuisance tripping will occur at IED6 and IED7 during a 3-phase SC fault at charger-Z terminal in the grid-connected case-2.

B. FAULTS DURING ISLANDED MODE

The islanded mode operation for the proposed AC Microgrid-1 will occur when the main grid is out of service, for example, due to the maintenance or fault on any part of connecting network. In the islanded mode with CB4 and CB5 open, both WTG and PV system are normally available to supply power to the cold-ironing and the harbor area loads during the daytime and only the WTG during the nighttime when the depleted vessel-BESS are being charged.

In the islanded mode it is required to operate the largest DER source like the WTG as the grid-forming DER while the smaller sources like PV system and if required the BESS at 0.69 kV harbor bus as the grid-following DERs according to IEEE Std. 1547.4-2011. In this regard, the DERs in the islanded mode are controlled in a manner to supply the required power to the harbor bus load and the cold-ironing load while maintaining the voltage and frequency at their terminals within the allowed limits. The WTG in the islanded mode operates as the grid-forming DER and both the PV system and BESS at 0.69 kV harbor bus operate as the grid-following DERs.

The same grid-connected OC settings are used for all IEDs in six islanded mode fault cases. The fault analysis and evaluation of selected OC settings of IEDs for six islanded mode

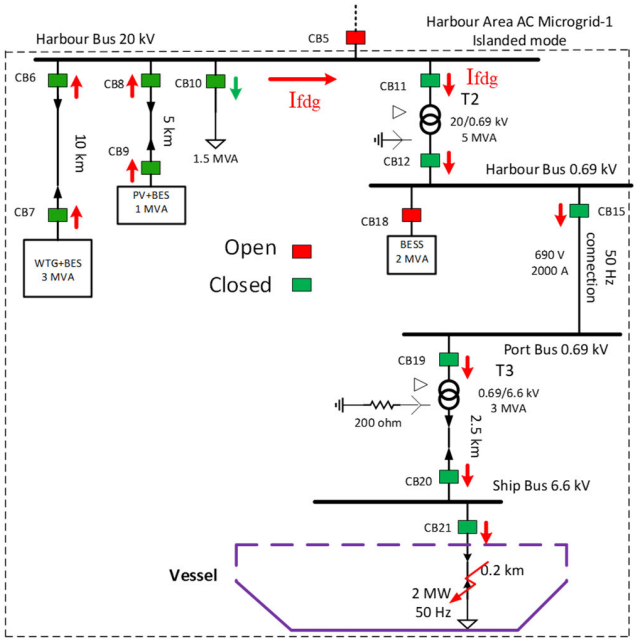

FIGURE 11. 3-phase short-circuit fault at 50 Hz cold-ironing load when supplied by WTG and PV during islanded mode 1.

cases with different scenarios of fault current contribution of DERs are explained in the next subsections. A 3-phase SC fault is applied for a duration of 4 s from the simulation time of 1.2 s to 5.2 s for most of the islanded mode cases, otherwise specified. The main purpose of all islanded mode cases is to check whether the fuses, primary OC IEDs and remote backup OC IEDs pick up and trip using the same grid-connected mode settings (2.5 x $I_{max-load}$) with different fault current contributions of DERs. If the answer is *YES*, then adaptive protection settings can be avoided in those islanded mode cases.

1) FAULTS AT 50 HZ COLD-IRONING LOAD WHEN WTG AND PV SUPPLY FAULT CURRENT

Fig.11 describes the islanded mode 1, where the green color indicates the closed or active IEDs and red color indicates the open or inactive IEDs. The combined fault current contribution of WTG and PV is denoted by I_{fdg}. The islanded mode 1 is further subdivided into two case studies: One related to fault current contribution of 1.2 p.u. from DERs and the other related to fault current contribution of 2 p.u. from DERs.

a: FULT CURRENT CONTRIBUTION OF 1.2 P.U. FROM DERs

Table 11 shows fault current magnitudes at all active IEDs in the fault path during a 3-phase SC fault at 50 Hz cold-ironing load in the islanded mode 1a. The fault current magnitudes at IEDs in Table 11 can be compared with maximum load currents (green-highlighted) of IEDs in Table 2-6. The results presented in Table 11 show that fault current magnitudes of 2.01-2.24 x $I_{max-load}$ are observed at IEDs 11-12, 15 and 19-21 in the islanded mode 1a that are lower than set OC

TABLE 11. Voltage and current at active IEDs during 3-phase short-circuit fault at 50 Hz cold-ironing load when supplied by WTG and PV during islanded mode 1A.

IED#	I (A)	V_{ph-ph} (kV)	IED#	I (A)	V_{ph-ph} (kV)
IED6	105.1	3.51	IED12	3780	0.084
IED7	103.75	3.89	IED15	3780	0.084
IED8	35	3.51	IED19	3780	0.084
IED9	34.5	3.61	IED20	395	0.0225
IED10	10.05	3.51	IED21	395	0.0225
IED11	130.5	3.51			

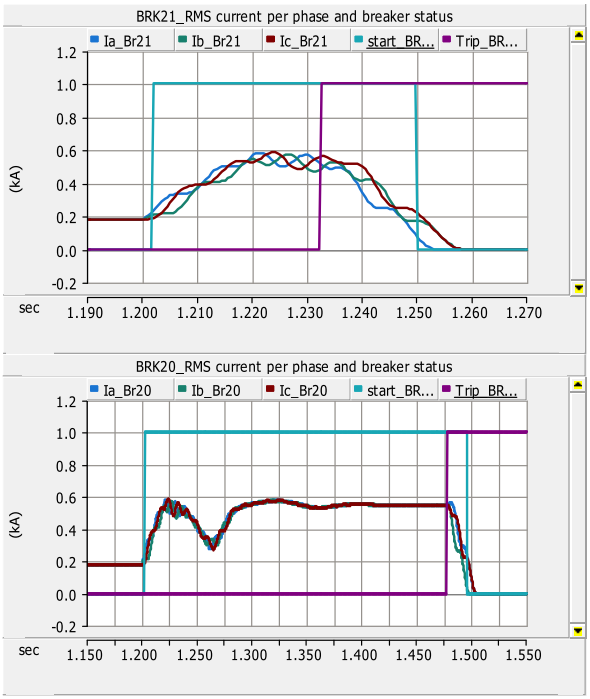

FIGURE 12. Magnitude of current per phase, pickup and tripping status of primary IED21 and backup IED20 during a 3-phase SC fault at 50 Hz cold-ironing load in islanded mode 1b.

tripping thresholds of 2.5 x $I_{max-load}$. This concludes that a fault current contribution of 1.2 p.u. from both WTG and PV system will not prevent adaptive OC settings in the islanded mode 1a. Only overload stages of IEDs will work in this mode.

b: FAULT CURRENT CONTRIBUTION OF 2 P.U. FROM DERs

Fig. 12 shows tripping responses of primary IED21 and backup IED20 during a 3-phase SC fault in the islanded mode 1b. Fig. 13 reveals that in the islanded mode 1b maximum fault current contribution comes from the nearest PV system and reduced fault current contribution comes from the WTG.

From Fig. 12 it is clear that IED21 trips within 32 ms of the 3-phase SC fault instead of the required tripping time of 20 ms (see Table 8). This means that the use of grid-connected mode settings in the islanded mode 1b causes 12 ms slower tripping response of primary IED21. This slower response of primary IED21 is due to the slower fault current ramp-up

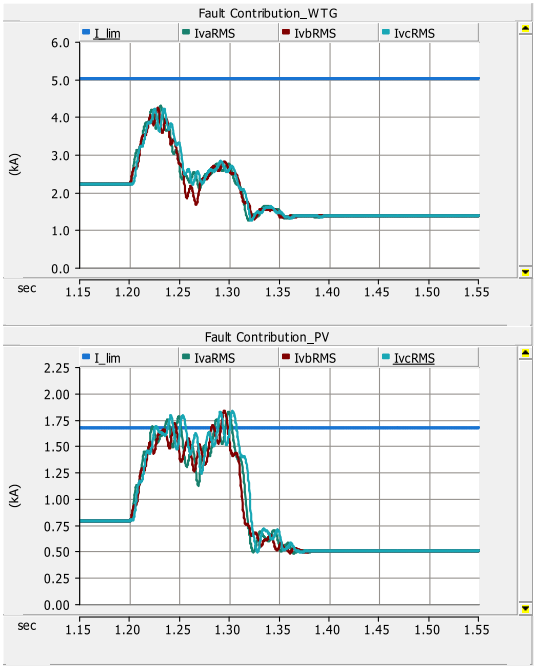

FIGURE 13. Magnitude of fault current contribution per phase by WTG and PV system during a 3-phase SC fault at 50 Hz cold-ironing load in islanded mode 1b.

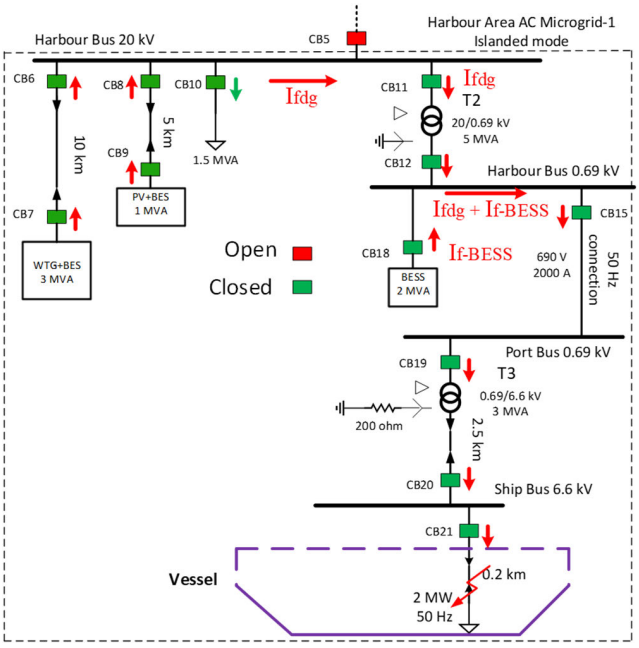

FIGURE 14. 3-phase short-circuit fault at 50 Hz cold-ironing load when supplied by WTG, PV and harbor-BESS during islanded mode 2.

time of DERs to reach to the required current level of the tripping threshold. The slower tripping responses of 75-79 ms are also observed at all backup IEDs in the fault path (IED20-19-15-12-11) that are set with a definite-time CTI of 200 ms between each primary IED and upstream backup IED. For example, Fig. 12 shows that after CB21 failure happens, the first backup IED20 will trip at simulation time of 1.475 s. It means the first backup IED20 will now trip within 275 ms instead of required 200 ms (20 ms + 180 ms) with a new CTI of 275-32 = 243 ms. In this case, the backup IED20 is 75 ms slower than set time delay. Despite the slower tripping response at each IED, the increased fault current contribution of 2 p.u. from DERs in the islanded mode 1b will potentially avoid adaptive OC settings during a 3-phase SC fault at 50 Hz cold-ironing load. For the sake of brevity, tripping responses of only primary IED and first backup IED are shown in Fig. 12.

2) FAULTS AT 50 HZ COLD-IRONING LOAD WHEN WTG, PV, AND HARBOR-BESS SUPPLY FAULT CURRENT

This is an extended case of the previous islanded mode 1 and in this case the BESS at 0.69 kV harbor bus is also used as a fault current source in addition to WTG and PV system during a 3-phase SC fault at 50 Hz cold-ironing load. In the islanded mode case 2 (Fig. 14) the BESS at 0.69 kV harbor bus is activated within 10 ms after the fault detection to provide extra fault current contribution. The purpose of connecting BESS is to check if the delayed tripping of primary IED21 and backup IEDs can be avoided.

The islanded mode 2 (Fig. 14) is further subdivided into three cases: First related to fault current contributions of 1.2 p.u. from harbor-BESS and 2 p.u. from DERs, second related to fault current contributions of 2 p.u. from harbor-BESS and DERs, and third related to fault current contributions of 3 p.u. from harbor-BESS and DERs. In Fig. 14, I_{fdg} denotes the combined fault current contribution from WTG and PV and I_{f-BESS} denotes the fault current contribution from BESS.

a: FAULT CURRENT CONTRIBUTION OF 1.2 P.U. FROM HARBOR-BESS AND 2 P.U. FROM THE WTG AND PV SYSTEM

Fig. 15 shows the tripping response of primary IED21 and backup IED20 during a 3-phase SC fault at 50 Hz cold-ironing load in the islanded mode 2a. Fig. 16 reveals that the maximum fault current contribution comes from the nearest DERs (BESS and PV system), and reduced fault current contribution comes from the distant WTG. From Fig. 15 it is clear that primary IED21 trips at simulation time of 1.232 s that is after 32 ms of the 3-phase SC fault instead of the required tripping time of 20 ms resulting in 12 ms slower tripping response in islanded mode 2a.

The first backup IED20 trips at simulation time of 1.458 s that is within an extended coordination time delay of 226 ms when IED21 or CB21 fails to trip. The second and third backups IED19 and IED15 trip within 201 ms and 196 ms coordination delay at simulation times of 1.659 s and 1.855 s, respectively. The fourth backup IED12 results in coordination delay of 217 ms because it trips at simulation time of 2.072 s instead of 2.055 s. The fifth backup IED11 trips at simulation time 2.271 s with 199 ms coordination delay. It is concluded

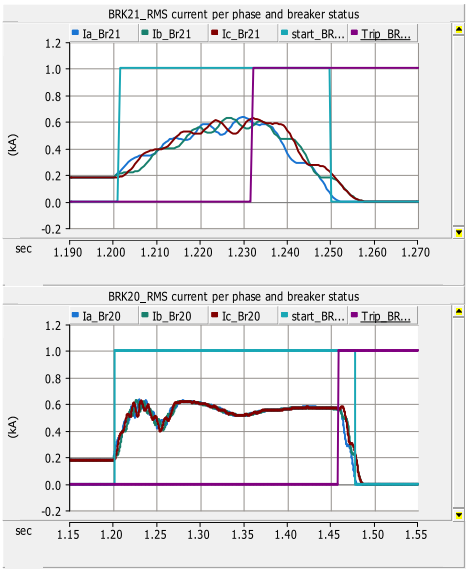

FIGURE 15. Magnitude of current per phase, pickup and tripping status of primary IED21 and backup IED20 during a 3-phase SC fault at 50 Hz cold-ironing load in islanded mode 2a.

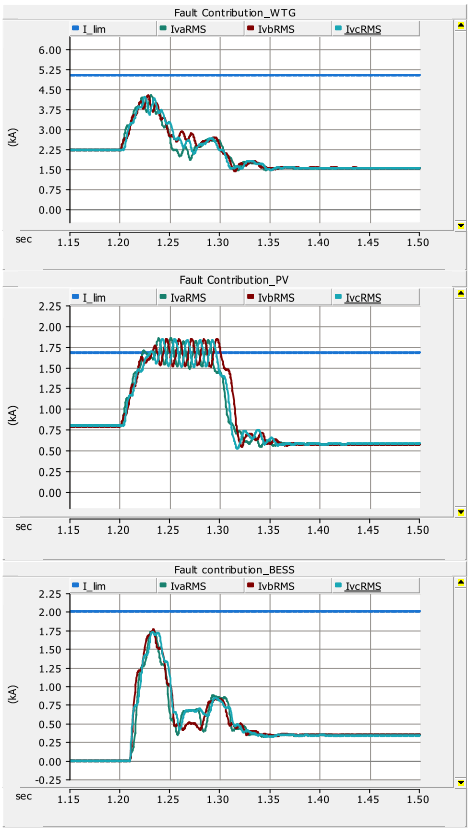

FIGURE 16. Magnitude of fault current contribution per phase by WTG, PV system and harbor-BESS during a 3-phase SC fault at 50 Hz cold-ironing load in islanded mode 2a.

that islanded mode 2a avoids both adaptive OC settings and slower tripping response of all backup IEDs in the fault path except primary IED21, backup IED20 and backup IED12.

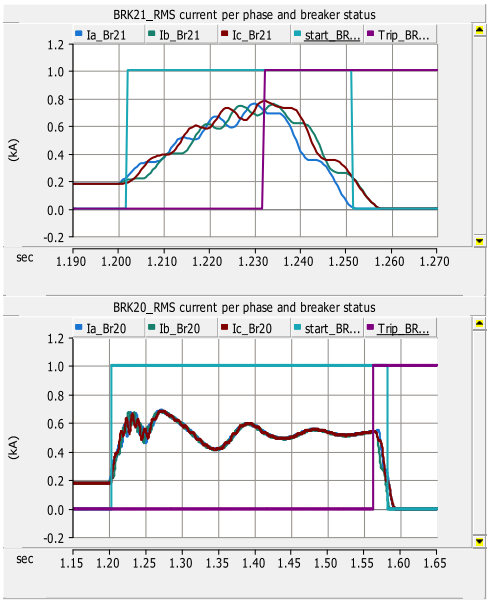

FIGURE 17. Magnitude of current per phase, pickup and tripping status of primary IED21 and backup IED20 during a 3-phase SC fault at 50 Hz cold-ironing load in islanded mode 2b.

b: FAULT CURRENT CONTRIBUTION OF 2 P.U. FROM THE WTG, PV SYSTEM, AND HARBOR-BESS

It is evident from Fig. 17 that in islanded mode 2b the tripping response of the primary IED21 is similar to that of the islanded mode 2a. The primary IED21 trips at simulation time of 1.232 s that is 12 ms slower than the required 20 ms tripping time. The first backup IED20 trips with new coordination time of 330 ms at simulation time of 1.562 s in islanded mode 2b (Fig. 17). The second and third backups IED19 and IED15 trip within 200 ms and 194 ms coordination delays at simulation times of 1.762 s and 1.956 s, respectively. The fourth and fifth backups IED12 and IED11 trip at simulation times of 2.065 s and 2.266s respectively resulting in respective coordination delays of 109 ms and 201 ms in islanded mode 2b. The fault current contributions of WTG, PV and harbor-BESS are presented in Fig. 18 for islanded mode 2b. The primary IED21 gives a similar tripping response irrespective of the fault current contribution of 1.2 p.u. or 2 p.u. from the harbor-BESS. It is concluded that in case 2b adaptive OC settings are avoided with similar coordination problems as in case 2a.

c: FAULT CURRENT CONTRIBUTION OF 3 P.U. FROM THE WTG, PV SYSTEM, AND HARBOR-BESS

From Fig. 19 it is clear that primary IED21 trips at simulation time of 1.232 s that is after 32 ms of the 3-phase SC fault resulting in 12 ms slower than required tripping response of 20 ms in islanded mode 2c. The first backup IED20 trips at simulation time of 1.412 s that is within the coordination delay of 180 ms when IED21 or CB21 fails to trip. Similarly, the second and third backups IED19 and IED15 trip within 200 ms coordination delays at simulation times of 1.612 s

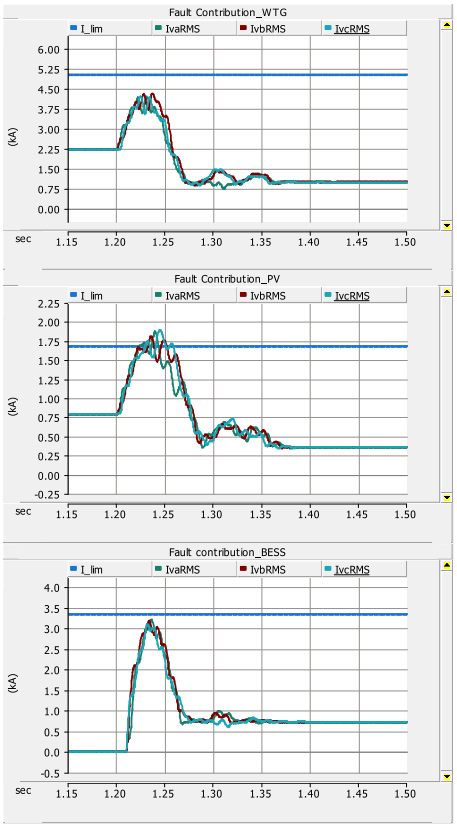

FIGURE 18. Magnitude of fault current contribution per phase by WTG, PV system and harbor-BESS during a 3-phase SC fault at 50 Hz cold-ironing load in islanded mode 2b.

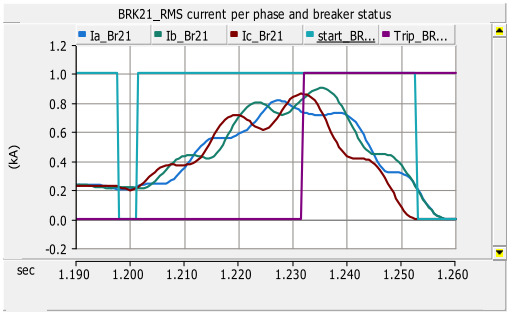

FIGURE 19. Magnitude of current per phase, pickup and tripping status of primary IED21 during a 3-phase SC fault at 50 Hz cold-ironing load in islanded mode 2c.

and 1.812 s, respectively. However, the fourth backup IED12 results in an extended coordination delay of 218 ms, that is 18 ms more than required because it trips at simulation time of 2.03 s instead of 2.012 s. The fifth backup IED11 trips at simulation time 2.23 s with 200 ms coordination delay. The results of only primary IED21 are shown in Fig. 19 and the rest of the results of islanded mode 2c are not shown for the sake of brevity. It is concluded that islanded mode 2c avoids both adaptive OC settings and slower tripping response of all backup IEDs in the fault path except one, the fourth backup IED12 that is delayed by 18 ms.

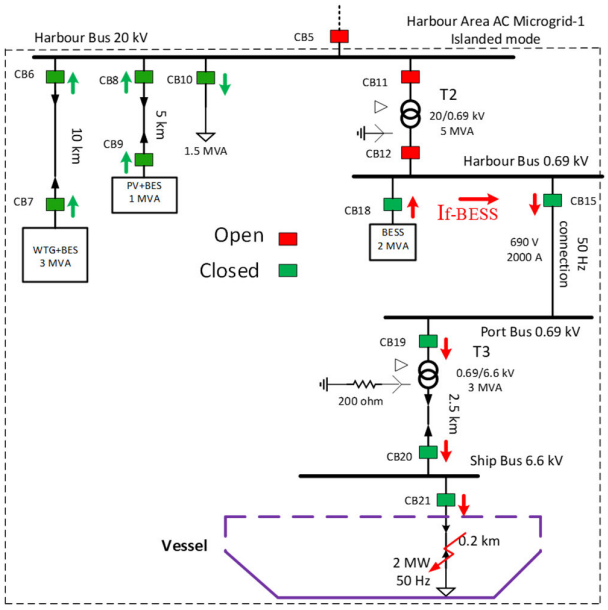

FIGURE 20. 3-phase short-circuit fault at 50 Hz cold-ironing load when supplied by only harbor-BESS during islanded mode 3.

3) FAULTS AT 50 HZ COLD-IRONING LOAD WHEN ONLY THE HARBOR-BESS SUPPLIES FAULT CURRENT

This case can be termed as an emergency case when the connection to WTG, PV system and related battery storages is lost in the islanded mode due to the fault at stepdown transformer T2 at 20 kV harbor bus. In this islanded mode 3 (Fig. 20) the BESS at 0.69 kV harbor bus can be used to supply 50 Hz cold-ironing load until the upstream fault is removed. The protection system in this case should also respond to any fault at or upstream to the cold-ironing load. Because only single DER source is available in this case so its fault current contribution should be enough to cause pickup and tripping of all the corresponding protection IEDs in the fault path.

The islanded mode 3 (Fig. 20) is further subdivided into two case studies: One related to fault current contribution of 2.5 p.u. from the harbor-BESS and the other related to fault current contribution of 3 p.u. from the harbor-BESS. In the islanded modes 3a and 3b, the duration of applied fault is 5.2 s from the simulation time of 1.2 s to the simulation time of 6.4 s to check if overload stages of IEDs also pick up and trip. Because the power rating of the cold-ironing load and the harbor-BESS is the same, that is 2 MW, therefore neither the fault current contribution of 1.2 p.u. nor the fault current contribution of 2 p.u. from the harbor-BESS will help avoiding adaptive OC settings of IED21. At 2 p.u. of the fault current contribution from harbor-BESS, only the overload stage of IED21 and backup IEDs will pick up and trip keeping the same OC settings as in the grid-connected mode.

a: FAULT CURRENT CONTRIBUTION OF 2.5 P.U. FROM HARBOR-BESS

Fig. 21 shows the tripping response of primary IED21 and backup IED20 during a 3-phase SC fault at 50 Hz

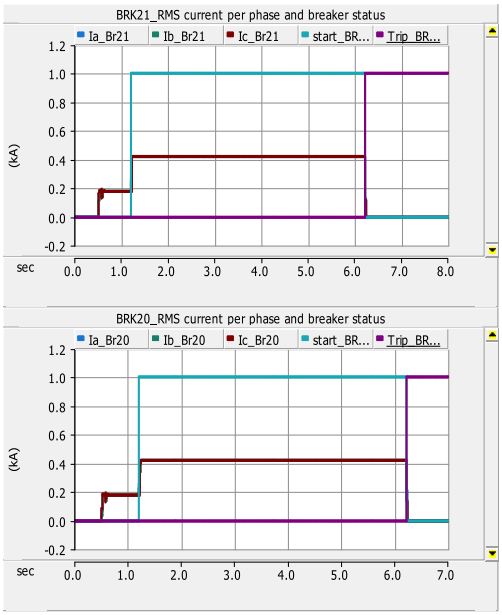

FIGURE 21. Magnitude of current per phase, pickup and tripping status of primary IED21 and backup IED20 during a 3-phase SC fault at 50 Hz cold-ironing load in islanded mode 3a.

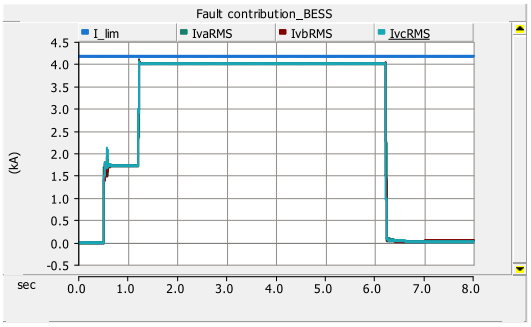

FIGURE 22. Magnitude of fault current contribution per phase by harbor-BESS during a 3-phase SC fault at 50 Hz cold-ironing load in islanded mode 3a.

cold-ironing load when harbor-BESS is set to provide fault current of 2.5 p.u. in islanded mode 3.

It is clear from Fig. 21 that only the overload stages of both primary IED21 and backup IED20 pick up and trip because harbor-BESS provides a fault current contribution of somewhat less than 2.5 p.u. in islanded mode 3a (Fig. 22). Therefore, fault current magnitudes observed at IED21 and IED20 are less than the corresponding OC setting thresholds of 2.5 $\times$ $I_{max-load}$. Other backup IEDs (IED19 and IED15) also give similar tripping response in this case. This concludes that fault current contribution of 2.5 p.u. from harbor-BESS will not avoid adaptive setting in islanded mode 3a.

b: FAULT CURRENT CONTRIBUTION OF 3 P.U. FROM HARBOR-BESS

It is observed that with a default rating or capacity of 2 MVA, the harbor-BESS is not capable of providing higher than

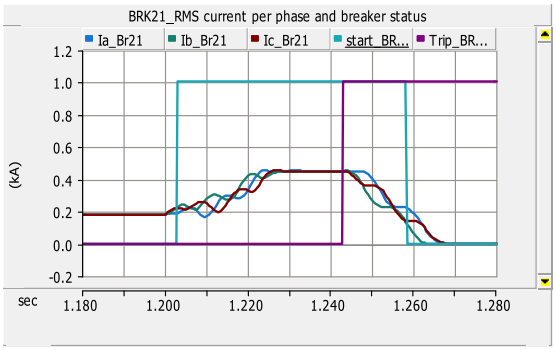

FIGURE 23. Magnitude of current per phase, pickup and tripping status of primary IED21 during a 3-phase SC fault at 50 Hz cold-ironing load when supplied by 2.2 MVA harbor-BESS in islanded mode 3b.

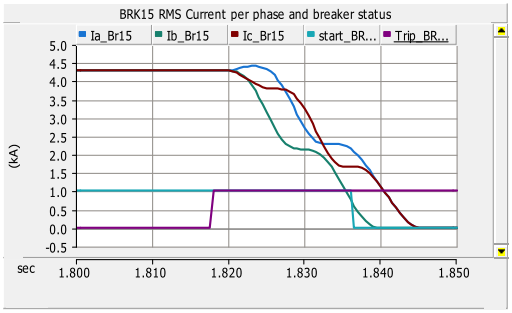

FIGURE 24. Magnitude of current per phase, pickup and tripping status of IED15 (third backup) during a 3-phase SC fault at 50 Hz cold-ironing load when supplied by 2.2 MVA harbor-BESS in islanded mode 3b.

2.5 p.u. of fault current contribution in the islanded mode 3b. It means that with a default rating the fault current contribution does not increase higher than that shown in Fig. 22 even if the maximum current limit (I-lim) is set as 3 p.u. Therefore, the tripping response of primary IED21, backup IED20 and other backup IEDs will be similar as in the previous islanded mode 3a (Fig. 21). However, with an increased rating or capacity of 2.2 MVA, the harbor-BESS is capable to provide enough fault current contribution to cause a pickup and tripping of primary IED21 during a 3-phase SC fault at 50 Hz cold-ironing load (Fig. 23). In this situation, only IED15 (third backup) will be capable of providing backup OC protection within 618 ms after the fault at simulation time of 1.818 s due to a sensed current of higher than its set tripping threshold of 2.5 $\times$ 1683 = 4207.5 A (see Fig. 24).

The results show that an additional installed capacity of 10 per cent of harbor-BESS will avoid adaptive OC settings with somehow slower tripping response (40 ms instead of 20 ms) of primary IED21 and limited backup OC protection only by IED15 in islanded mode 3b. The fault current contribution of 2.2 MVA harbor-BESS in islanded mode 3b is shown in Fig. 25. An additional installed capacity of 25 per cent of harbor-BESS (2 MVA+0.5 MVA) will avoid adaptive OC settings, reduce primary IED21 tripping response to 30 ms and ensure all backup IEDs (IED20, 19 and 15) pick up and trip in case of CB21 failure.

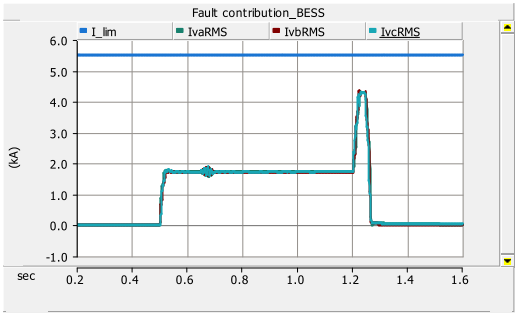

FIGURE 25. Magnitude of fault current contribution per phase by 2.2 MVA harbor-BESS during a 3-phase SC fault at 50 Hz cold-ironing load in islanded mode 3b.

4) FAULTS AT CHARGER-Z TERMINAL WHEN ONLY THE WTG SUPPLIES FAULT CURRENT

In this islanded mode only the WTG supplies power to the harbor load of 1.5 MW and three depleted vessel-BESS each of 2 MWh rated capacity. The islanded mode 4 (Fig. 26) happens when the connection to the main grid is lost during the nighttime when depleted vessel-BESS are on slow charging. This mode assumes that only the WTG is available with its full rated capacity of 3 MW and PV system together with its storage (PV+BES) is out of service. With only the WTG in service supplying the rated power not only the load at harbor area can be supplied but also a power demand of 0.6 MW for slow charging of depleted vessel-BESS can easily be met in addition to some power losses. Various types of faults may happen in this mode, but the most important type of fault is at the terminals of the battery chargers. Since the battery chargers using power electronics components are relatively costly components so their fault protection is very important. The battery chargers are protected by using both the fast-acting full-range fuses and the fast-acting breakers operated by backup IEDs. Because all of the three battery chargers (charger-X, Y and Z) are identical in capacity and construction, therefore only the faults at one charger location (charger-Z) have been analyzed.

The islanded mode 4 (Fig. 26) is further subdivided into three case studies: One related to fault current contribution of 1.2 p.u. (islanded mode 4a), the second related to fault current contribution of 2 p.u. (islanded mode 4b) and third related to fault current contribution of 3 p.u. (islanded mode 4c) from the WTG. The main purpose of selecting different fault current levels of the WTG is to check proper operation of fuses and backup IEDs during 3-phase SC fault. In islanded modes 4a-4c, the duration of applied fault is 5.2 s from the simulation time of 1.2 s to the simulation time of 6.4 s to check whether overload stages of IEDs also pick up and trip.

a: FAULT CURRENT CONTRIBUTION OF 1.2 P.U. FROM THE WTG

Table 12 shows magnitudes of currents and voltages at all active IEDs during a 3-phase SC fault at charger-Z terminal in islanded mode 4a. The results show that fault current

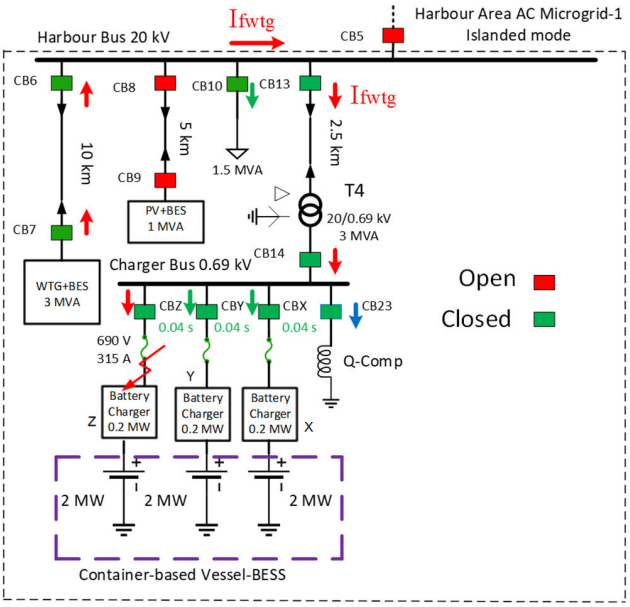

FIGURE 26. 3-phase short-circuit fault at Charger-Z terminal when supplied by only WTG during islanded mode 4.

TABLE 12. Voltage and current at active IEDs during 3-phase short-circuit fault at charger-Z terminal in islanded mode 4A.

IED#	I (A)	$V_{ph\text{-}ph}$ (V)	IED#	I (A)	$V_{ph\text{-}ph}$ (V)
IED6	105	1200	IED14	2980	20
IED7	104	1760	IEDX	80	20
IED10	3.5	1200	IEDY	80	20
IED13	102	1200	IEDZ	3000	Zero

magnitudes at the first backup IEDZ, the second backup IED14 and the third backup IED13 are greater than the set thresholds of 2.5 x $I_{max-load}$ at these IEDs. Therefore, IEDZ, IED14 and IED13 can easily trip after 0.04 s, 0.24 s and 0.44 s of the 3-phase SC fault at charger-Z terminal assuming a coordination delay of 0.2 s between each backup IED. The primary protection is provided by the fast acting fuse that is disabled in simulation to test the tripping of backup IEDs.

Fig. 27 shows magnitudes of currents per phase, pickup and tripping signals of IEDZ and IED14 during a 3-phase SC fault at charger-Z terminal in islanded mode 4a. The first backup IEDZ trips within the required 40 ms of the SC fault at simulation time of 1.24 s and the second backup IED14 also picks up to provide backup protection if IEDZ fails to trip due to any reason.

Fig. 28 reveals that the fast acting fuseZ at charger-Z terminal blows within 255 ms at simulation time of 1.455 s after the occurrence of 3-phase SC fault at simulation time of 1.2 s in islanded mode 4a. Fault current contribution of WTG during islanded mode 4a is shown in Fig. 29. The results show that in islanded mode 4a, the tripping response of fuseZ (primary OC protection) is 215 ms slower than the first backup IEDZ that trips within 40 ms of the 3-phase SC fault. The slower tripping response of fuse is unacceptable in islanded mode 4a because it creates coordination problem

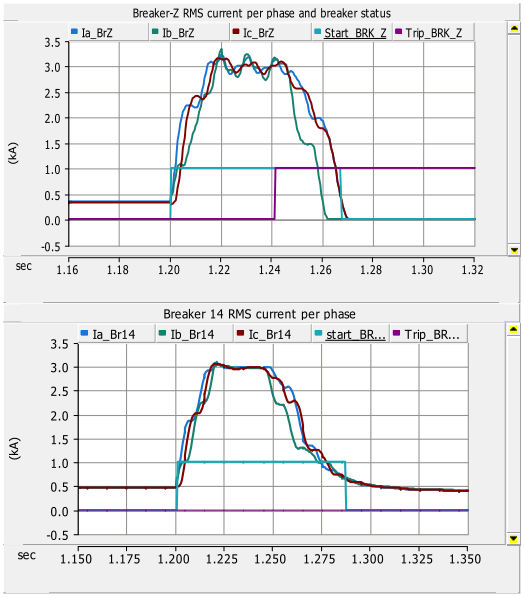

FIGURE 27. Magnitude of current per phase, pickup and tripping status of IEDZ (first backup) and IED14 (second backup) during a 3-phase SC fault at charger-Z terminal in islanded mode 4a.

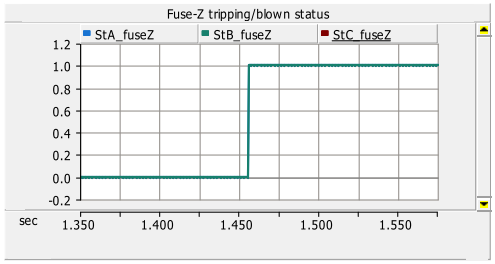

FIGURE 28. Status/tripping response of fuseZ during a 3-phase SC fault at charger-Z terminal in islanded mode 4a.

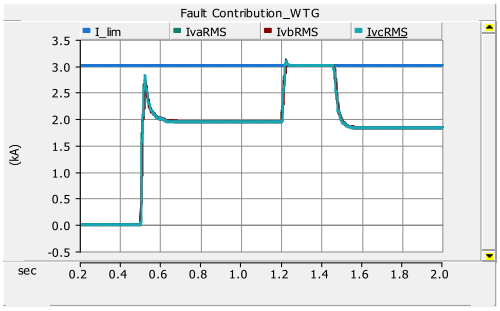

FIGURE 29. Magnitude of fault current contribution per phase by the WTG during a 3-phase SC fault at charger-Z terminal in islanded mode 4a.

between the primary OC protection (fuseZ) and backup OC protection IEDZ. For a proper protection coordination, the fuse needs to operate within 20 ms after the 3-phase SC fault instead of 255 ms. This concludes that the islanded mode 4a avoids adaptive protection settings but creates the coordination problem between fuseZ and backup IEDZ.

b: FAULT CURRENT CONTRIBUTION OF 2 P.U. FROM THE WTG

Fig. 30 reveals that the fast acting fuseZ at charger-Z terminal blows within 105 ms at simulation time of 1.305 s after the

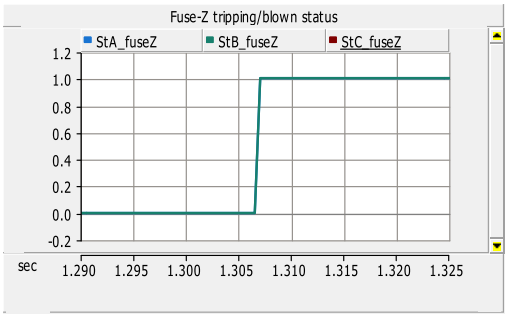

FIGURE 30. Status/tripping response of fuseZ during a 3-phase SC fault at charger-Z terminal in islanded mode 4b.

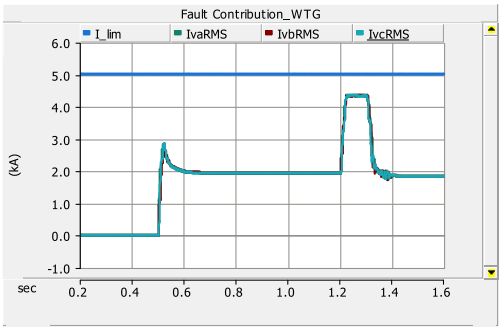

FIGURE 31. Magnitude of fault current contribution per phase by the WTG during a 3-phase SC fault at charger-Z terminal in islanded mode 4b.

occurrence of 3-phase SC fault at simulation time of 1.2 s in islanded mode 4b. It means that in islanded mode 4b, the tripping response of fuseZ (primary OC protection) is 65 ms slower than the first backup IEDZ that trips within 40 ms of the 3-phase SC fault. The obvious reason of slower than expected 20 ms tripping response of fuseZ is less than the required magnitude of fault current sensed by the fusing element due to less than 2 p.u. fault current contribution of the WTG (Fig. 31) in the islanded mode 4b due to the network impedance. Although the tripping response of fuseZ is improved in the islanded mode 4b compared with the islanded mode 4a, it still creates coordination problem between fuseZ and the first backup IEDZ.

c: FAULT CURRENT CONTRIBUTION OF 3 P.U. FROM THE WTG

Fig. 32 shows that fuseZ blows with a time delay of 33 ms when a 3-phase SC fault is applied at simulation time of 1.2 s in the islanded mode 4c. Although the tripping response of fuseZ is still 13 ms slower than the expected 20 ms, but 3 p.u. fault current contribution from the WTG will maintain protection coordination between fuseZ and first backup IEDZ though with only a coordination time delay of 7 ms between them. For more speedy tripping response of fuseZ to maintain the required coordination delay of 20 ms between fuseZ and IEDZ, the WTG must provide a fault current contribution of more than 3 p.u. Alternately, the coordination time delay between fuseZ and IEDZ should be extended from 20 ms to 40 ms.

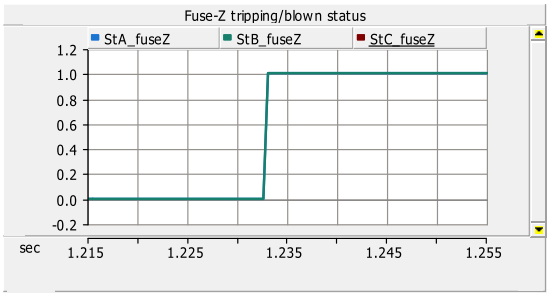

FIGURE 32. Status/tripping response of fuseZ during a 3-phase SC fault at charger-Z terminal in islanded mode 4c.

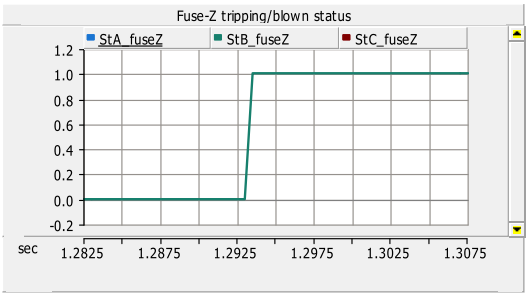

FIGURE 34. Status/tripping response of fuseZ during a 3-phase SC fault at charger-Z terminal in islanded mode 5a.

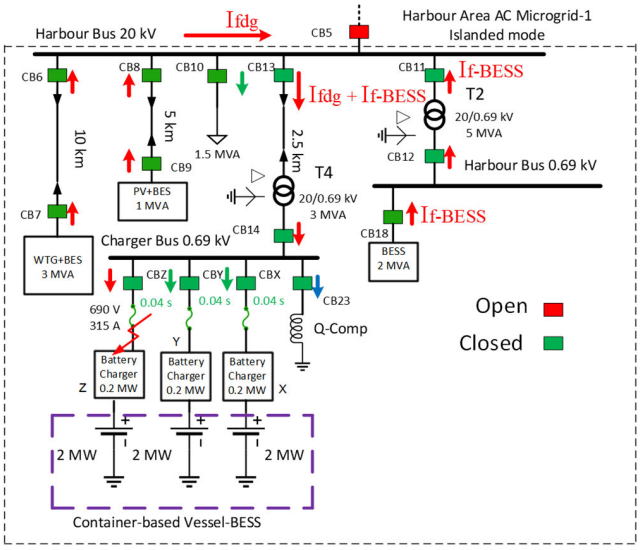

FIGURE 33. 3-phase short-circuit fault at charger-Z terminal when supplied by WTG, PV-BES and harbor-BESS during islanded mode 5.

5) FAULTS AT CHARGER-Z TERMINAL WHEN WTG, PV-BES, AND HARBOR-BESS SUPPLY FAULT CURRENT

This is an extended case for the previous islanded mode 4. In the islanded mode 5 (Fig. 33), it is checked if the fuseZ operates as fast as in the grid-connected mode during 3-phase SC fault at Charger-Z terminal when the battery energy storage at PV system (PV-BES) and BESS at 0.69 kV harbor bus are also activated within 10 ms as extra fault-current sources. The main purpose of the islanded mode 5 is to check whether protection coordination between fuseZ and IEDZ can be maintained using existing available fault current sources with different levels of fault current contributions. Hence, the tripping response of only fuseZ is presented in the results because IEDZ trips within required 40 ms even with 1.2 p.u. fault current contribution of the WTG (case 4a). Same is the case for other backup IEDs in the fault path.

The islanded mode 5 (Fig. 33) is further subdivided into four case studies: The first related to fault current contribution of 1.2 p.u. from the WTG, PV-BES and harbor-BESS, the second related to the fault current contribution of 2 p.u. from the WTG, PV-BES and harbor-BESS, the third related to the fault current contribution of 3 p.u. from the WTG and 2 p.u. from the PV-BES and harbor-BESS, and the fourth related to the fault current contribution of 2.5 p.u. from the WTG, PV-BES and harbor-BESS.

a: FAULT CURRENT CONTRIBUTION OF 1.2 P.U. FROM THE WTG, PV-BES, AND HARBOR-BESS

Fig. 34 reveals that the fast acting fuseZ at charger-Z terminal blows within 92.5 ms at the simulation time of 1.2925 s after the occurrence of 3-phase SC fault at simulation time of 1.2 s in islanded mode 5a. It means that the tripping response of fuseZ (primary OC protection) is 72.5 ms slower than expected 20 ms when each of the WTG, PV-BES and harbor-BESS provides a fault current contribution of 1.2 p.u. (Fig. 35). In this case, the first backup IEDZ will trip before fuseZ. Therefore, it can be concluded that fault current contribution of 1.2 p.u. from the DERs is not enough for maintaining a proper protection coordination between fuseZ and backup IEDZ in the islanded mode 5a.

b: FAULT CURRENT CONTRIBUTION OF 2 P.U. FROM THE WTG, PV-BES, AND HARBOR-BESS

Fig. 36 reveals that the fast acting fuseZ at charger-Z terminal blows within 53 ms at simulation time of 1.253 s after the occurrence of 3-phase SC fault at simulation time of 1.2 s in islanded mode 5b. It means that the tripping response of fuseZ (primary OC protection) is 33 ms slower than expected 20 ms when each of the WTG, PV-BES and harbor-BESS is set to provide a fault current contribution of 2 p.u. Fig. 37 shows that the fault current contribution of the distant WTG is somehow limited to less than 2 p.u. due to the increased fault current contribution from the nearby PV-BES and harbor-BESS in comparison to the islanded mode 5a. It can be concluded that a fault current contribution of 2 p.u. from the DERs is not enough for maintaining a proper protection coordination between fuseZ and backup IEDZ in the islanded mode 5b.

c: FAULT CURRENT CONTRIBUTION OF 3 P.U. FROM THE WTG, AND 2 P.U. FROM THE PV-BES AND THE HARBOR-BESS

Fig. 38 reveals that the fast acting fuseZ at charger-Z terminal blows within 18 ms at simulation time of 1.2175 s after the

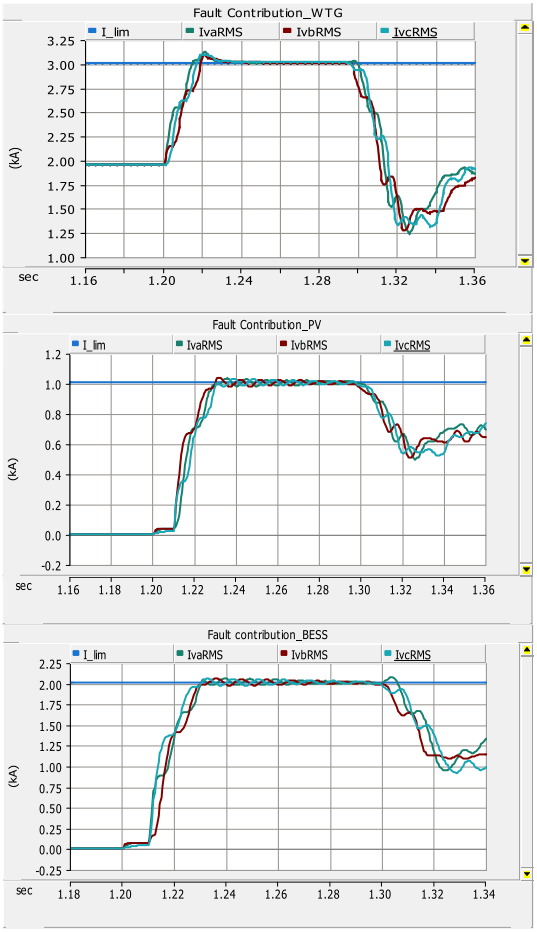

FIGURE 35. Magnitude of fault current contribution per phase by the WTG. PV-BES and harbor-BESS during a 3-phase SC fault at charger-Z terminal in islanded mode 5a.

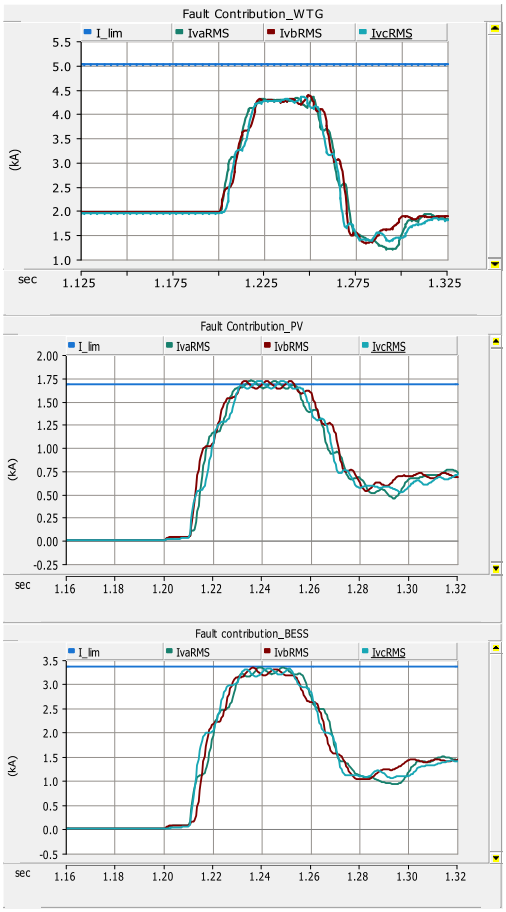

FIGURE 37. Magnitude of fault current contribution per phase by the WTG. PV-BES and harbor-BESS during a 3-phase SC fault at charger-Z terminal in islanded mode 5b.

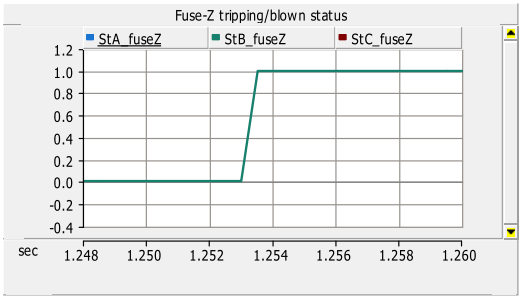

FIGURE 36. Status/tripping response of fuseZ during a 3-phase SC fault at charger-Z terminal in islanded mode 5b.

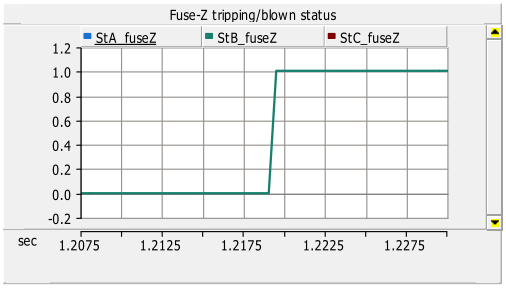

FIGURE 38. Status/tripping response of fuseZ during a 3-phase SC fault at charger-Z terminal in islanded mode 5c.

occurrence of 3-phase SC fault at simulation time of 1.2 s in islanded mode 5c. It means that the tripping response of fuseZ (primary OC protection) is 2 ms faster than the expected 20 ms when the WTG is set to provide fault current contribution of 3 p.u. and both PV-BES and harbor-BESS are set to provide a fault current contribution of 2 p.u. It is concluded that a proper protection coordination between fuseZ and backup IEDZ in the islanded mode 5c is maintained at the mentioned fault current contributions.

d: FAULT CURRENT CONTRIBUTION OF 2.5 P.U. FROM THE WTG, PV-BES AND HARBOR-BESS

Fig. 39 reveals that the fast acting fuseZ at charger-Z terminal blows within 17 ms at simulation time of 1.217 s after the occurrence of 3-phase SC fault at simulation time of 1.2 s in islanded mode 5d. It means that the tripping response of fuseZ (primary OC protection) is 3 ms faster than the expected 20 ms when the WTG, PV-BES and harbor-BESS are set to provide a fault current contribution of 2.5 p.u. Fig. 40 shows the fault current flowing through fuseZ in the islanded

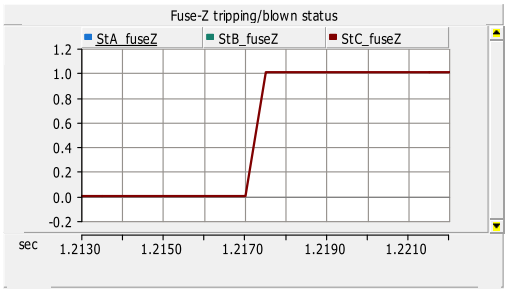

FIGURE 39. Status/tripping response of fuseZ during a 3-phase SC fault at charger-Z terminal in islanded mode 5d.

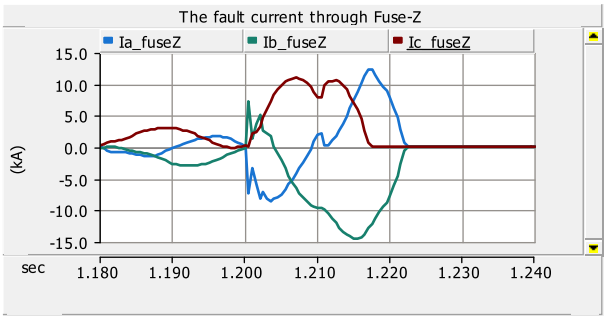

FIGURE 40. Magnitude of fault current per phase flowing through fuseZ during a 3-phase SC fault at charger-Z terminal in islanded mode 5d.

mode 5d. It is concluded that a proper protection coordination between fuseZ and backup IEDZ in the islanded mode 5d is maintained at the mentioned fault current contributions.

6) FAULTS AT CHARGER-Z TERMINAL WHEN WTG, HARBOR-BESS, AND HEALTHY CHARGING VESSEL-BESS SUPPLY FAULT CURRENT

This is an extended case for the previous islanded case 5. In this case 6 (Fig. 41) not only the WTG and harbor-BESS can be used but also the healthy container-based vessel-BESS on charge can be utilized as the extra fault-current sources during the non-availability of PV-BES. For this purpose, 0.2 MW chargers of container-based vessel-BESS need to be bidirectional type providing 1.2-3 p.u. of the rated discharging current during 3-phase SC faults for practical application in the islanded mode 6.

In the islanded mode 6, the battery chargers X and Y along with 2 MWh batteries are replaced with generic DER models each of 0.2 MVA capacity to emulate their discharging mode. The main purpose of the islanded mode 6 is to check if the protection coordination between fuseZ and IEDZ can be maintained using the mentioned fault current sources with different levels of fault current contributions.

The islanded mode 6 (Fig. 41) is further subdivided into four case studies (6a-6d) according to different fault current contributions of DERs as discussed in the following subsections. In all of the four case studies of the islanded mode 6, the harbor-BESS, vessel-BESS-X, and vessel-BESS-Y are activated with a delay of 10 ms after the fault.

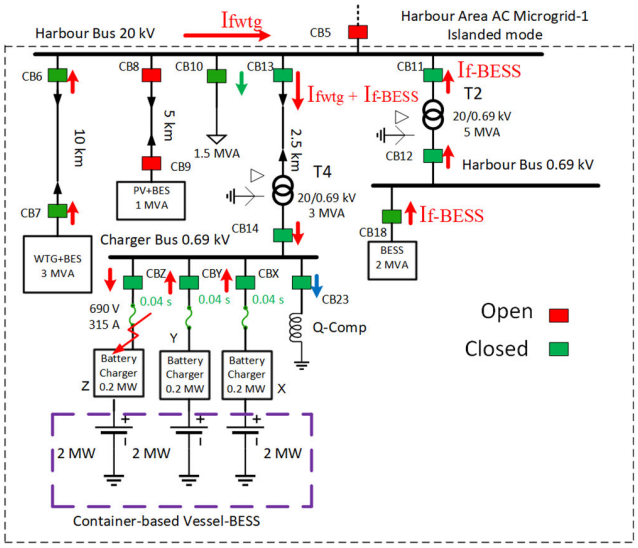

FIGURE 41. 3-phase short-circuit fault at Charger-Z terminal when supplied by WTG, harbor-BESS and healthy container-based vessel-BESS during islanded mode 6.

a: FAULT CURRENT CONTRIBUTION OF 1.2 P.U. FROM THE WTG, HARBOR-BESS, VESSEL-BESS-X, AND VESSEL-BESS-Y

Fig. 42 reveals that the fast acting fuseZ at charger-Z terminal blows within 101 ms at simulation time of 1.301 s after the occurrence of 3-phase SC fault at simulation time of 1.2 s in islanded mode 6a. It means that the tripping response of fuseZ (primary OC protection) is 81 ms slower than expected 20 ms when each of the WTG, harbor-BESS, vessel-BESS-X, and vessel-BESS-Y provides a fault current contribution of 1.2 p.u. It can be concluded that a fault current contribution of 1.2 p.u. from DERs is not enough for maintaining a proper protection coordination between fuseZ and backup IEDZ in the islanded mode 6a because backup IEDZ will trip before the fuseZ blows.

b: FAULT CURRENT CONTRIBUTION OF 2 P.U. FROM THE WTG, HARBOR-BESS, VESSEL-BESS-X, AND VESSEL-BESS-Y

Fig. 43 reveals that the fast acting fuseZ at charger-Z terminal blows within 36 ms at simulation time of 1.236 s after the occurrence of 3-phase SC fault at simulation time of 1.2 s in islanded mode 6b. It means that the tripping response of fuseZ (primary OC protection) is 16 ms slower than expected 20 ms when each of the WTG, harbor-BESS, vessel-BESS-X, and vessel-BESS-Y provides a fault current contribution of 2 p.u. It can be concluded that a fault current contribution of 2 p.u. from DERs is not enough for maintaining a proper protection coordination between fuseZ and backup IEDZ in the islanded mode 6b because the coordination time delay has become very short (only 4 ms instead of 20 ms).

c: FAULT CURRENT CONTRIBUTION OF 2.5 P.U. FROM THE WTG, HARBOR-BESS, VESSEL-BESS-X, AND VESSEL-BESS-Y

Fig. 44 reveals that the fast acting fuseZ at charger-Z terminal blows within 37 ms at simulation time of 1.237 s after the occurrence of 3-phase SC fault at simulation time of 1.2 s in

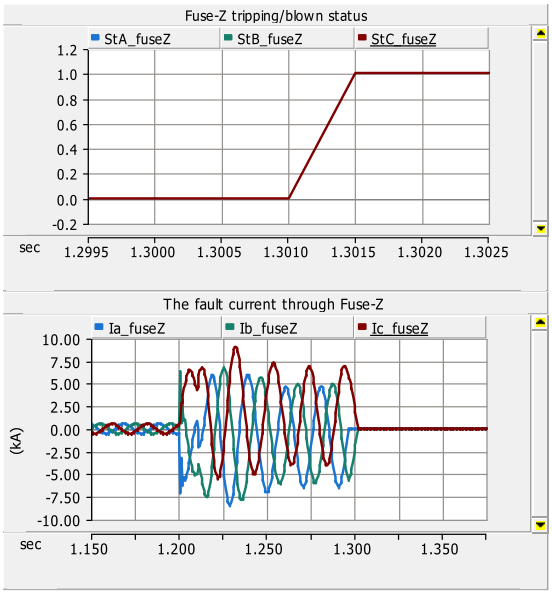

FIGURE 42. Status/tripping response of fuseZ (top) and magnitude of fault current per phase flowing through fuseZ (bottom) during a 3-phase SC fault at charger-Z terminal in islanded mode 6a.

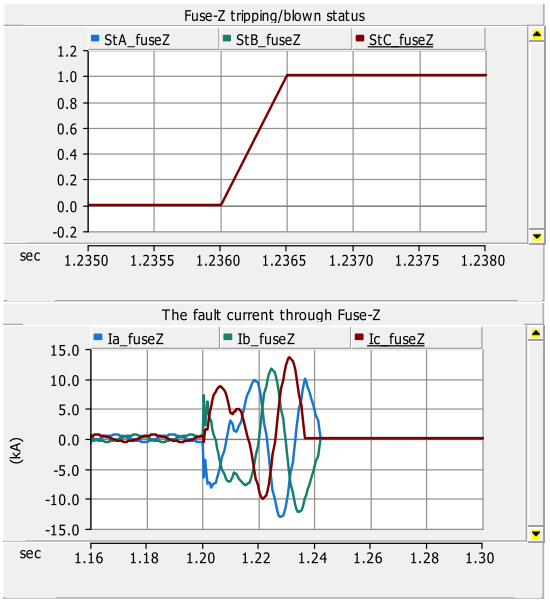

FIGURE 43. Status/tripping response of fuseZ (top) and magnitude of fault current per phase flowing through fuseZ (bottom) during a 3-phase SC fault at charger-Z terminal in islanded mode 6b.

islanded mode 6c. It means that the tripping response of fuseZ (primary OC protection) is 17 ms slower than expected 20 ms when each of the WTG, harbor-BESS, vessel-BESS-X, and vessel-BESS-Y is set to provide a fault current contribution of 2.5 p.u. This is due to the fact that in the islanded mode 6c, less than the set limit of fault current contribution from DERs is observed. It can be concluded that a fault current contribution of 2.5 p.u. from DERs is not enough for maintaining a proper protection coordination between fuseZ and backup IEDZ in

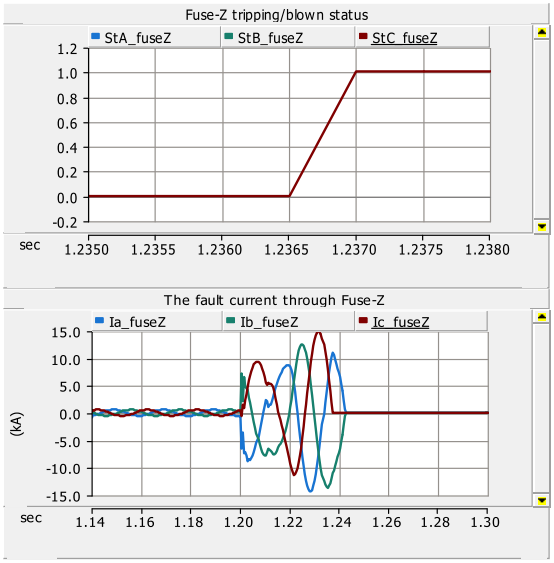

FIGURE 44. Status/tripping response of fuseZ (top) and magnitude of fault current per phase flowing through fuseZ (bottom) during a 3-phase SC fault at charger-Z terminal in islanded mode 6c.

the islanded mode 6c because the coordination time delay has become very short (only 3 ms instead of 20 ms).

d: FAULT CURRENT CONTRIBUTION OF 3 P.U. FROM THE WTG, HARBOR-BESS, VESSEL-BESS-X, AND VESSEL-BESS-Y

Fig. 45 reveals that the fast acting fuseZ at charger-Z terminal blows within 36 ms at simulation time of 1.236 s after the occurrence of 3-phase SC fault at simulation time of 1.2 s in islanded mode 6d. It means that the tripping response of fuseZ (primary OC protection) is 16 ms slower than expected 20 ms when each of the WTG, harbor-BESS, vessel-BESS-X, and vessel-BESS-Y is set to provide a fault current contribution of 3 p.u. This is due to the fact that in the islanded mode 6d, less than the set limit of fault current contribution from DERs is observed. It can be concluded that a fault current contribution of 3 p.u. from DERs is not enough for maintaining a proper protection coordination between fuseZ and backup IEDZ in the islanded mode 6d because the coordination time delay has become very short (only 4 ms instead of 20 ms).

The results show that the only way for maintaining a proper coordination in the islanded modes 6b, 6c and 6d is to increase the coordination time delay between fuseZ and backup IEDZ from the existing 20 ms coordination time delay to the new 40 ms coordination time delay. In this way, only a fault current contribution of 2 p.u. from DERs will be sufficient for the proper protection coordination, detection and isolation of 3-phase SC fault at charger-Z terminal in the islanded mode 6. There are two obvious and unavoidable time delays resulting in the slow tripping/blowing response of fuseZ in islanded mode cases 6a-6d. One is the activation time delay of 10 ms taken by extra fault current sources. The second is the ramp-up time delay of fault currents provided by DERs to reach up to their maximum values for fuse to respond.

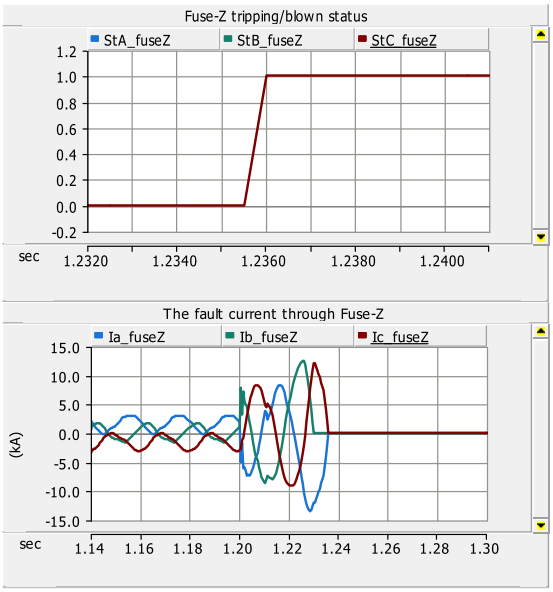

FIGURE 45. Status/tripping response of fuseZ (top) and magnitude of fault current per phase flowing through fuseZ (bottom) during a 3-phase SC fault at charger-Z terminal in islanded mode 6d.

III. DISCUSSION

Table 13 presents the summary of the islanded mode fault cases for the harbor area AC microgrid-1. The islanded mode cases 1a to 3b are related to 3-phase SC fault at the cold-ironing load whereas the islanded mode cases 4a to 6d are related to 3-phase SC fault at charger-Z terminal. In the islanded mode cases 1a to 3b it is checked if adaptive OC settings can be avoided and protection coordination between the primary and backup IEDs in the fault path can be properly maintained. In the islanded mode cases 4a to 6d the operating time of fast acting fuse is also checked in addition to avoidance of adaptive OC settings and maintenance of proper protection coordination between IEDs in the fault path.

From the summary in Table 13 and results in Table 14 it is evident that in most of the islanded mode cases adaptive OC settings can be avoided with different combinations of fault current contributions of DERs except in islanded mode cases 1a, 3a and 3b. The exceptional islanded cases 1a, 3a and 3b are obvious islanded modes with either minimum magnitudes of fault current contributions from DERs or minimum number/capacity of DERs. The adaptive OC settings can only be avoided in the exceptional islanded mode case 1a by increasing fault current contributions of DERs as done in case 1b, and in exceptional islanded mode cases 3a and 3b by adding 25 per cent extra MVA capacity.

The results indicate that in most of the islanded mode cases, the tripping time of primary IED or fuse is delayed which results in subsequent extended coordination delays between the backup IEDs. In islanded mode cases 4c, 6b, 6c and 6d the operating time of fuseZ is delayed up to 20 ms or less, therefore, a revised coordination delay of 40 ms instead of existing 20 ms between fuseZ and the first backup IEDZ may solve the coordination problem. This requires some compromise on backup IEDs' operations. In exceptional islanded cases 1a, 3a and 3b, the protection coordination between IEDs can be improved by increasing fault current contributions of DERs, using only the grid-forming control of all DERs and adding 25 per cent extra MVA capacity.

Last but not least, the avoidance of adaptive OC protection settings, the maintenance of protection coordination, and the operation of fuse within 20 ms are possible by using existing available DERs and battery storages as fault current sources during 3-phase SC fault in islanded mode cases 2c, 5c and 5d. The only concern will be to disconnect the extra

TABLE 13. Summary of islanded mode fault cases of the harbor area AC microgrid-1.

Islanded mode fault case	Fault current contribution from DERs	Are adaptive OC settings avoided?	Is protection coordination maintained?	Does fuse operate within 20 ms?
1a	WTG: 1.2 p.u. PV: 1.2 p.u.	NO	NO	-
1b	WTG: 2 p.u. PV: 2 p.u.	YES	YES (PARTIALLY)[1]	-
2a	WTG: 2 p.u. PV: 2 p.u. H-BESS: 1.2 p.u.	YES	YES (PARTIALLY)	-
2b	WTG: 2 p.u. PV: 2 p.u. H-BESS: 2 p.u.	YES	YES (PARTIALLY)	-
2c	WTG: 3 p.u. PV: 3 p.u. H-BESS: 3 p.u	YES	YES	-
3a	H-BESS: 2.5 p.u.	NO	NO	-
3b	H-BESS: 3 p.u.	NO	NO	-
		YES (25% additional MVA capacity)	YES (25% additional MVA capacity)	-
4a	WTG: 1.2 p.u.	YES	YES (PARTIALLY)	NO (Delayed)
4b	WTG: 2 p.u.	YES	YES (PARTIALLY)	NO (Delayed)
4c	WTG: 3 p.u.	YES	YES (PARTIALLY)*	NO (Delayed)**
5a	WTG: 1.2 p.u. PV-BES: 1.2 p.u. H-BESS: 1.2 p.u	YES	YES (PARTIALLY)	NO (Delayed)
5b	WTG: 2 p.u. PV-BES: 2 p.u. H-BESS: 2 p.u	YES	YES (PARTIALLY)	NO (Delayed)
5c	WTG: 3 p.u. PV-BES: 2 p.u. H-BESS: 2 p.u	YES	YES	YES
5d	WTG: 2.5 p.u. PV-BES: 2.5 p.u. H-BESS: 2.5 p.u	YES	YES	YES
6a	WTG: 1.2 p.u. H-BESS: 1.2 p.u. V-BESS: 1.2 p.u.	YES	YES (PARTIALLY)	NO (Delayed)
6b	WTG: 2 p.u. H-BESS: 2 p.u. V-BESS: 2 p.u.	YES	YES (PARTIALLY)*	NO (Delayed)**
6c	WTG: 2.5 p.u. H-BESS: 2.5 p.u. V-BESS: 2.5 p.u.	YES	YES (PARTIALLY)*	NO (Delayed)**
6d	WTG: 3 p.u. H-BESS: 3 p.u. V-BESS: 3 p.u.	YES	YES (PARTIALLY)*	NO (Delayed)**

WTG=Wind turbine generator, PV = Photovoltaic, BESS = Battery energy storage system
H-BESS = Harbor-BESS, PV-BES = PV-Battery energy storage,
V-BESS = Vessel-BESS (both X and Y), MVA = Mega Volt-Ampere.
*Can be improved by extending coordination delay between fuseZ and IEDZ to 40 ms
**FuseZ operating time is delayed up to 20 ms or less.
[1] Grid -forming control of both WTG and PV will improve the coordination delay of primary and backup IEDs closer to the setting limits in the islanded mode 1b.

TABLE 14. Operating times of IEDs in islanded mode fault cases.

Fault Cases	Operating times (ms) during 3-phase SC faults										
	IED21		IED20	IED19		IED15		IED12		IED11	
1a	I>@5		I>@5	I>@5		I>@5		I>@5		I>@5	
1b	32		275	477		675		879		1079	
2a	32		258	459		655		872		1071	
2b	32		362	562		756		865		1066	
2c	32		212	412		612		830		1030	
3a	I>@5		I>@5	I>@5		I>@5		-			
3b	40		I>@5	I>@5		618					
→	4a	4b	4c	5a	5b	5c	5d	6a	6b	6c	6d
FuseZ	255	105	33	92.5	53	17.5	17	101	36	37	36
IEDZ	40*	ms = Millisecond, SC = Short-circuit, I>@5 = Overload stage operating in 5 s.									
IED14	240*	→ Fault cases in columns, IEDs in rows.									
IED13	440*	*IEDZ, IED14 and IED13 have same operating times in cases 4a-6d.									

Primary protection devices are highlighted in green, and backups are highlighted in blue color.

activated fault current sources immediately after the fault is isolated to prevent overvoltage and related aftereffects like AC microgrid's instability or blackout due to disconnection of the required DERs by the overvoltage protection.

In general, adaptive OC protection settings may still be required for the islanded mode AC microgrids protected by the inverse-time OC function. This conclusion can be easily drawn from the results of islanded mode 6 as the operation of fuseZ, that is an inverse-time OC device, is delayed in all four cases. However, a separate coordination study for the inverse-time OC function will confirm whether the adaptive protection will be required, or it can avoided for the considered islanded modes with different scenarios of fault current contributions of converter-based DERs.

IV. CONCLUSION

The magnitudes of maximum load currents and the short-circuit fault currents at each IED during the grid-connected and islanded modes of harbor area AC microgrid-1 have been determined. The operating time and protection coordination of definite-time OC relays and fast acting fuse during the selected 3-phase SC faults in the grid-connected mode have been evaluated and found to be correct according to the settings. The evaluation of operating time and protection coordination of definite-time OC relays and fast acting fuse during the selected 3-phase SC faults for six islanded mode cases with different fault current contributions of DERs have also been done. It is found that grid-connected mode settings of definite-time OC can also be effectively used during 3-phase SC faults in the islanded modes if the active/operational DERs and freely-available quickly operated battery storage units provide at least 3 p.u. of fault current contribution. In this way adaptive definite-time OC settings can be avoided, and proper definite-time protection coordination and fast fuse operation can be ensured during 3-phase SC faults in the islanded modes of AC microgrid.

REFERENCES

[1] K. Marquart, T. Haasdijk, G. B. Ferrari, and R. Schmidhalter. (2010). Reprint ABB Review 4/2010 Shore-to-Ship Power. ABB, Switzerland, Accessed: Nov. 20, 2017. [Online]. Available: https://library.e.abb.com/public/8f916bbe49d92d1ac12579680032f273/Shore-to-ship-power-2010-low.pdf

[2] J. Kumar, O. Palizban, and K. Kauhaniemi, "Designing and analysis of innovative solutions for Harbour area smart grid," in *Proc. IEEE Manchester PowerTech*, Manchester, U.K., Jun. 2017, pp. 1–6.

[3] J. Kumar, A. A. Memon, L. Kumpulainen, K. Kauhaniemi, and O. Palizban, "Design and analysis of new Harbour grid models to facilitate multiple scenarios of battery charging and onshore supply for modern vessels," *Energies*, vol. 12, no. 12, p. 2354, Jun. 2019, doi: 10.3390/en12122354.

[4] *Utility connections in port—Part 1: High Voltage Shore Connection (HVSC) Systems—General requirements*, document IEC/ISO/IEEE 80005-1, Ed. 2.0, International Electrotechnical Commission, Geneva, Switzerland, Mar. 2019, pp. 1–74. [Online]. Available: www.iec.ch

[5] D. W. Gao, E. Muljadi, T. Tian, M. Miller, and W. Wang, "Comparison of standards and technical requirements of grid-connected wind power plants in China and the United States," Nat. Renew. Energy Lab. (NREL), Golden, CO, USA, Tech. Rep. NREL/TP-5D00-64225, Sep. 2016.

[6] *Requirements for Generating Plants to be Connected in Parallel With Distribution Networks. Part 1: Connection to a LV Distribution Network. Generating Plants up to and Including Type B*, Standard SFS-EN 50549-1:2019, European Committee for Electrotechnical Standardization, Brussels, Belgium, Feb. 2019, pp. 1–71.

[7] *Requirements for Generating Plants to be Connected in Parallel With Distribution Networks. Part 2: Connection to a MV Distribution Network. Generating Plants up to and Including Type B*, Standard SFS-EN 50549-2:2019, European Committee Electrotechnical Standardization, Brussels, Belgium, Feb. 2019, pp. 1–80.

[8] *IEEE Standard for Interconnection and Interoperability of Distributed Energy Resources With Associated Electric Power Systems Interfaces*, Standard IEEE 1547-2018, IEEE Standards Association, IEEE Standards Coordinating Committee 21, Feb. 2018, pp. 1–136.

[9] *IEEE Guide for Design, Operation, and Integration of Distributed Resource Island Systems with Electric Power Systems*, IEEE Standard 1547.4-2011, IEEE Standards Association, IEEE Standards Coordinating Committee 21, Jul. 2011, pp. 1–42.

[10] *IEEE Standard for the Specification of Microgrid Controllers*, IEEE Standard 2030.7-2017, IEEE Standards Association, IEEE Standards Coordinating Committee 21, Dec. 2017, pp. 1–41.

[11] *Amendment 1 Utility connections in Port—Part 1: High Voltage Shore Connection (HVSC) Systems—General Requirements*, document IEC/ISO/IEEE 80005-1:2019/AMD1:2022, Ed. 2.0, International Electrotechnical Commission, Geneva, Switzerland, Feb. 2022, pp. 1–7. [Online]. Available: https://www.iec.ch

[12] *Utility Connections in Port—Part 3: Low Voltage Shore Connection (LVSC) Systems—General Requirements*, document IEC/ISO/IEEE PAS 80005-3:2014, Ed. 1.0, International Electrotechnical Commission, Geneva, Switzerland, Aug. 2014, pp. 1–51. [Online]. Available: https://www.iec.ch

[13] A. A. Memon and K. Kauhaniemi, "A critical review of AC microgrid protection issues and available solutions," *Electric Power Syst. Res.*, vol. 129, pp. 23–31, Dec. 2015, doi: 10.1016/j.epsr.2015.07.006.

[14] A. A. Memon, H. Laaksonen, and K. Kauhaniemi, "Microgrid protection with conventional and adaptive protection schemes," in *Microgrids*, A. Anvari-Moghaddam, H. Abdi, B. Mohammadi-Ivatloo, and N. Hatziargyriou, Eds. Cham, Switzerland: Springer, 2021, ch. 19, pp. 523–579, doi: 10.1007/978-3-030-59750-4_19.

[15] A. A. Memon and K. Kauhaniemi, "An adaptive protection for radial AC microgrid using IEC 61850 communication standard: Algorithm proposal using offline simulations," *Energies*, vol. 13, no. 20, p. 5316, Oct. 2020.

[16] H. Laaksonen, D. Ishchenko, and A. Oudalov, "Adaptive protection and microgrid control design for Hailuoto island," *IEEE Trans. Smart Grid*, vol. 5, no. 3, pp. 1486–1493, May 2014, doi: 10.1109/TSG.2013.2287672.

[17] J. Niiranen, R. Komsi, M. Routimo, T. Lähdeaho, and S. Antila, "Experiences from a back-to-back converter fed village microgrid," in *Proc. IEEE PES Innov. Smart Grid Technol. Conf. Eur. (ISGT Europe)*, Gothenburg, Sweden, Oct. 2010, pp. 1–5.

[18] M. Ferrari and L. M. Tolbert, "Inverter design with high short-circuit fault current contribution to enable legacy overcurrent protection for islanded microgrids," in *Proc. IEEE Power Energy Soc. Gen. Meeting (PESGM)*, Denver, CO, USA, Jul. 2022, pp. 1–5.

[19] A. Cruden and G. J. W. Dudgeon, "The impact of energy storage devices used in conjunction with renewable embedded generators, on the protection and control system," in *Proc. 7th Int. Conf. Develop. Power Syst. Protection (DPSP)*, Amsterdam, The Netherlands, Apr. 2001, pp. 230–233.

[20] P. Nuutinen, P. Peltoniemi, and P. Silventoinen, "Short-circuit protection in a converter-fed low-voltage distribution network," *IEEE Trans. Power Electron.*, vol. 28, no. 4, pp. 1587–1597, Apr. 2013, doi: 10.1109/TPEL.2012.2213845.

[21] S. Gupta, S. Mukhopadhyay, A. Banerji, and S. K. Biswas, "Fault management in isolated microgrid," in *Proc. IEEE Int. Conf. Power Electron., Drives Energy Syst. (PEDES)*, Chennai, India, Dec. 2018, pp. 1–6.

[22] A. H. Etemadi and R. Iravani, "Overcurrent and overload protection of directly voltage-controlled distributed resources in a microgrid," *IEEE Trans. Ind. Electron.*, vol. 60, no. 12, pp. 5629–5638, Dec. 2013, doi: 10.1109/TIE.2012.2229680.

[23] K. O. Oureilidis and C. S. Demoulias, "A fault clearing method in converter-dominated microgrids with conventional protection means," *IEEE Trans. Power Electron.*, vol. 31, no. 6, pp. 4628–4640, Jun. 2016, doi: 10.1109/TPEL.2015.2476702.

[24] L. Qi, M. Carminati, and M. Riva, "Fault interruption and protection coordination in converter interfaced distribution systems," in *Proc. IEEE Power Energy Soc. Gen. Meeting (PESGM)*, Portland, OR, USA, Aug. 2018, pp. 1–5.

[25] C.-H. Noh, C.-H. Kim, G.-H. Gwon, M. O. Khan, and S. Z. Jamali, "Development of protective schemes for hybrid AC/DC low-voltage distribution system," *Int. J. Electr. Power Energy Syst.*, vol. 105, pp. 521–528, Feb. 2019, doi: 10.1016/j.ijepes.2018.08.030.

[26] D. B. Rathnayake, M. Akrami, C. Phurailatpam, S. P. Me, S. Hadavi, G. Jayasinghe, S. Zabihi, and B. Bahrani, "Grid forming inverter modeling, control, and applications," *IEEE Access*, vol. 9, pp. 114781–114807, 2021, doi: 10.1109/ACCESS.2021.3104617.

[27] N. Mohammed, H. H. Alhelou, and B. Bahrani, *Grid-Forming Power Inverters: Control and Applications*, 1st ed. Boca Raton, FL, USA: CRC Press, 2023, [Online]. Available: https://www.taylorfrancis.com/, doi: 10.1201/9781003302520.

[28] A. Yazdani and R. Iravani, "Controlled-frequency VSC system," in *Voltage-Sourced Converters in Power Systems: Modeling, Control, and Applications*, vol. 9. Hoboken, NJ, USA: Wiley, 2010, pp. 245–269.

[29] *Technical Catalogue PCS100 SFC Static Frequency Converter, 2UCD030000E009_d PCS100 SFC Technical Catalogue*, ABB Limted, New Zealand, 2021, Accessed: Dec. 13, 2022, pp. 1–35. [Online]. Available: https://library.e.abb.com/public/65b31251075443f09c54549966809657/2UCD030000E009_d%20PCS100%20SFC%20Technical%20Catalogue.pdf

AUSHIQ ALI MEMON (Member, IEEE) received the B.E. degree in electrical engineering from the Quaid-e-Awam University of Engineering, Science and Technology, Nawabshah, Pakistan, in 2006, and the M.Sc. degree in electrical power engineering from the Brandenburg University of Technology, Cottbus, Germany, in 2013. He is currently pursuing the Ph.D. degree with the Department of Electrical Engineering, University of Vaasa, Finland. Previously, he was a Lecturer with the Quaid-e-Awam University of Engineering, Science and Technology, from 2007 to 2009. He was a Project Researcher with the University of Vaasa, from 2014 to 2020. His research interests include power system protection, microgrids, power system transient simulations, smart grids, and power electronics applications.

KIMMO KAUHANIEMI (Member, IEEE) received the M.S. and Ph.D. degrees in electrical engineering from the Tampere University of Technology, Finland, in 1987 and 1993, respectively. Previously, he was with ABB Corporate Research and the VTT Technical Research Centre, Finland. He is currently with the University of Vaasa, where he is a Professor of electrical engineering and leads the Smart Electric Systems Research Group. His research interests include power system transient simulation, protection of power systems, grid integration of distributed generation, and microgrids.